minerals

MDPI

Article

The Concentration of Nickel and Cobalt from Agios Ioannis Laterites by Multi-Gravity Separator

Amina Eljoudiani [1,*], Moacir Medeiros Veras [1,2], Carlos Hoffmann Sampaio [1], Josep Oliva Moncunill [1], Stylianos Tampouris [3] and Jose Luis Cortina Pallas [4]

[1] Departament d'Enginyeria Minera, Industrial i TIC, Escola Politècnica Superior d'Enginyeria de Manresa, Universitat Politècnica de Catalunya, Av. Bases de Manresa 61-63, 08242 Manresa, Spain; moacir.medeiros@upc.edu or moacir.veras@ifap.edu.br (M.M.V.); carlos.hoffmann@upc.edu (C.H.S.); josep.oliva@upc.edu (J.O.M.)
[2] Instituto Federal de Educação, Ciência e Tecnologia do Amapá, Macapá 68909-398, Brazil
[3] GMMSA LARCO Fragkoklissias 27, 15125 Athens, Greece; stelios.tabouris@larco.gr
[4] Departament d'Enginyeria Química, Campus Diagonal Besòs, Edifici I, Eduard Maristany, 16, Sant Andrá de Besòs, 08930 Barcelona, Spain; jose.luis.cortina@upc.edu
* Correspondence: amina.eljoudiani@upc.edu

Abstract

Asbolane is a secondary source of cobalt (Co) and manganese (Mn), essential for battery and alloy production. Enhancing the utilization of low-grade ores, typically containing ~1.2% Co and 14.7% Mn, is vital for conserving high-grade resources. However, fine grinding for such ores presents challenges for conventional gravity separation. This study investigates the effectiveness of the Multi-Gravity Separator (MGS) in processing finely disseminated asbolane ore from Agios Ioannis, Greece. The study was conducted at the Mineral Processing Laboratory of UPC/Bases Manresa. Two size fractions, D_{80} (−100 +50 µm and −50 µm), were tested under varying drum speeds, tilt angles, and wash water flows. Response surface methodology (RSM) was implemented using Python-optimized (version 3.15) process parameters. The results demonstrate that a concentrate with 2.6% Co and 32.5% Mn can be obtained, achieving 82.1% Co recovery. Independent and multi-objective optimizations confirm MGS as a viable method for recovering Co and Mn from complex low-grade ores, with reduced overgrinding-related energy losses essential for production. The study aimed to implement and enhance low-grade asbolane ore from a feed containing 2.6% Co and 32.5% Mn. Variables were optimized with a multi-objective target, demonstrating their effectiveness.

Keywords: asbolane; cobalt; manganese; nickel; low-grade ores; high-performance alloys; gravity separation; Multi-Gravity Separator (MGS)

check for updates

Academic Editor: Manoj Khanal

Received: 29 May 2025
Revised: 27 June 2025
Accepted: 30 June 2025
Published: 4 July 2025

Citation: Eljoudiani, A.; Medeiros Veras, M.; Sampaio, C.H.; Moncunill, J.O.; Tampouris, S.; Cortina Pallas, J.L. The Concentration of Nickel and Cobalt from Agios Ioannis Laterites by Multi-Gravity Separator. *Minerals* **2025**, *15*, 714. https://doi.org/10.3390/min15070714

Copyright: © 2025 by the authors. Licensee MDPI, Basel, Switzerland. This article is an open access article distributed under the terms and conditions of the Creative Commons Attribution (CC BY) license (https://creativecommons.org/licenses/by/4.0/).

1. Introduction

The global demand for critical metals such as cobalt (Co) and nickel (Ni) has risen sharply, driven by their indispensable roles in the aerospace and electronics industries' clean-energy technologies, rechargeable batteries, and advanced materials [1]. The recovery of strategic metals, particularly nickel and cobalt, from laterite ores is of increasing interest due to their importance in key technological sectors, such as lithium-ion batteries, aeronautics, and the specialty alloys industry [1]. Nevertheless, laterites, one of the primary sources of nickel and cobalt, pose metallurgical challenges due to their mineralogical complexity and varied mineral phases [2].

Lateritic deposits, such as those in Agios Ioannis, Greece, are among the world's primary sources of cobalt and nickel. These deposits, however, present significant challenges for metal recovery due to their complex mineralogy and the ultrafine nature of valuable particles [3]. Due to poor selectivity and low recoveries, the particle size range between −100 and +50 microns is challenging to process using conventional beneficiation methods like flotation or magnetic separation [4].

Mineral Liberation Analysis (MLA) is an essential technique for evaluating the distribution and association of mineral phases in ores [3]. It allows for alterations in the degree of liberation of valuable minerals to optimize concentration and extraction processes [5]. This technique was applied in this study of the Agios Ioannis laterite to assess the liberation of asbolane, a mineral containing nickel, cobalt, and manganese [6].

MLA revealed that asbolane exhibits significant liberation in the Agios Ioannis laterite [7,8]. The distribution of asbolane grains indicates a partial to complete liberation, suggesting the potential for efficient extraction of its contained metals [9]. The liberated asbolane particles are predominantly fine to medium-sized, which may influence flotation and leaching parameters [10].

In terms of composition, asbolane is a complex mineral primarily containing nickel (Ni), cobalt (Co), and manganese (Mn) [11]. Its presence in laterite as a distinct liberated phase allows for targeted beneficiation strategies to maximize metal recovery [12]. The association of asbolane with other mineral phases has also been analyzed, revealing coexistence with iron oxides and phyllosilicates, which may influence extractive process choices [13]. Thus, applying MLA to the Agios Ioannis laterite highlights the significance of asbolane as a source of strategic metals and paves the way for optimized extraction approaches [14].

Among the different methods for laterite enrichment, advanced gravity separation, particularly the use of the MGS, has been studied for its efficiency in recovering nickel- and cobalt-bearing minerals, especially in the fine fractions of the ores [15].

Previous studies have demonstrated that the MGS is particularly suitable for treating fine particles, significantly improving metal recovery from lateritic ores [16,17]. This technology offers a good balance between selectivity and recovery by applying combined gravitational and centrifugal force. Furthermore, MGS has been shown to effectively separate complex oxide ores containing high-value elements, as seen in the study by Das et al. Additionally, its application to polymetallic ores by Angadi et al. has confirmed its effectiveness in separating nickel- and cobalt-bearing minerals. Moreover, as a physical separation method, MGS presents notable environmental advantages over chemical processes, such as reduced reagent use and lower waste generation.

MGS utilizes centrifugal force combined with a shaking motion to create a highly selective separation environment, capable of efficiently recovering fine and ultrafine particles based on differences in specific gravity and surface properties. MGS is particularly suitable for treating fine laterite ores, where traditional methods struggle to achieve meaningful separation [18,19]. The technique's adaptability to fine-particle beneficiation has been demonstrated in various mineral systems, offering opportunities to enhance the recovery of cobalt and nickel from fine-grained lateritic fractions [20].

The lateritic ore bodies at Agios Ioannis are marked by a complex mineralogical composition, where economically significant metals such as cobalt and nickel are hosted within silicate and oxide matrices. These metals are typically finely disseminated throughout the ore, especially within the intermediate particle size range of −100 µm to +50 µm. This fraction poses considerable processing challenges, as it is frequently associated with reduced recovery efficiency when treated through conventional beneficiation methods. Consequently, this size range is often underutilized or discarded during processing [20].

A critical factor influencing the success of beneficiation is the degree of mineral liberation, defined as the separation of valuable mineral phases from gangue material during the comminution stage. Incomplete liberation frequently results in lower recovery rates and diminished concentrate quality. In the Agios Ioannis deposit, the intergrowth of cobalt- and nickel-bearing phases with various silicate and oxide minerals significantly complicates their liberation and subsequent separation.

Notably, asbolane represents an exception within this mineralogical system. It typically occurs in a liberated form, enabling its more efficient recovery. In contrast, most cobalt- and nickel-bearing phases remain locked within the ore matrix, particularly in the problematic particle size fraction between −100 µm and +50 µm. Despite the potential metal value within this fraction, it is commonly excluded from processing streams due to its detrimental effect on overall recovery performance [20].

The Multi-Gravity Separator (MGS) has emerged as an effective technique for processing lateritic ores, particularly due to its high efficiency in recovering ultrafine particles that often host significant concentrations of valuable nickel and cobalt minerals. Unlike conventional gravity separation methods such as shaking tables or spiral concentrators, the MGS combines centrifugal force with a transverse shaking motion, allowing for an improved separation of particles with only slight differences in specific gravity [21]. In a comparative analysis, Nnaemeka Stanislaus and Nzeh et al. [22] observed that the MGS improved nickel recovery by up to 30% compared to spiral concentrators when treating fine laterite tailings. Moreover, MGS offers a more environmentally friendly and energy-efficient alternative to pressure acid leaching (HPAL) and other hydrometallurgical processes, which typically require high energy inputs and aggressive chemical reagents [22]. Yldiz et al. [23] further demonstrated that MGS outperformed flotation and traditional centrifugal concentrators regarding selectivity and overall recovery in the beneficiation of lateritic ores.

This study investigates the potential of MGS technology to selectively recover cobalt and nickel from the laterite ores of Agios Ioannis, especially the nickel and cobalt contained in the mineral asbolane, a manganese oxyhydroxide. Two specific particle size fractions are examined: the D_{80} (−100 µm +50 µm) fraction and the D_{80} (−50 µm) fraction, to evaluate the influence of particle size on the performance of the MGS. Key operational parameters, including feed rate, rotational speed, tilt angle, and wash water flow, were optimized to achieve maximum recovery and grade for cobalt and nickel. The novelty of this study lies in its systematic application of MGS technology to ultrafine lateritic ore fractions, specifically targeting asbolane-hosted metals, which have not been extensively explored in prior literature. By integrating mineralogical analyses with process performance data, this research comprehensively evaluates MGS technology's applicability in processing fine lateritic ores, to enhance the economic viability of cobalt and nickel recovery.

2. Materials and Methods

2.1. Description of the Equipment

The MGS is an advanced gravity-based separation device designed to recover fine and ultrafine particles based on density differentials. Previous studies have demonstrated its efficacy in processing particles below 100 µm [21–29]. In the current investigation, a C900 pilot-scale MGS unit was employed.

The MGS integrates centrifugal acceleration with a superimposed sinusoidal vibration to generate a dynamic, thin-film stratification environment that enables enhanced density separation. The core components and operational sequence of the MGS unit are outlined as follows (Figure 1):

(a) Rotating Drum Assembly [27]

The central cylindrical drum is inclined at a shallow angle (2°–5°) and rotates at speeds between 170 and 330 rpm. This motion produces a moderate centrifugal force equivalent to 5–15 g, which promotes the radial migration of denser particles. The drum's internal surface is lined with concentric mesh rings (1–3 mm apertures), which establish a particle stratification zone and aid in retaining heavier particles during separation.

(b) Shaking Mechanism

The unit employs a sinusoidal vibration system, oscillating longitudinally at 4–8 Hz with an adjustable stroke length of 10–20 mm. This vibration periodically fluidizes the slurry film, enhancing particle stratification by specific gravity and increasing the separation resolution between mineral phases.

(c) Feed and Wash Water System

The feed slurry is introduced via a calibrated distributor at the elevated end of the drum. Wash water is applied counter-currently through evenly spaced spray bars along the drum length, typically at 1–2 bar pressures and flow rates of 5–15 L/min. This setup ensures continuous renewal of the film layer and facilitates the removal of lighter gangue material.

(d) Separation Process

Feed slurry forms a thin film (2–5 mm thick) across the internal drum surface. Under the combined effects of centrifugal and oscillatory forces, heavier mineral particles migrate outward through the mesh rings and settle toward the drum wall. In comparison, lighter particles remain suspended and are carried toward the discharge end. This configuration allows for separating particles down to 1 μm, which are otherwise difficult to recover using conventional gravity methods.

(e) Product Collection System

Separated heavy particles (concentrate) are scraped off by adjustable internal blades and collected in a dedicated launder. Depending on operating parameters, the mass yield of the focus typically ranges from 5% to 25% of the feed. The tailings stream, composed primarily of lighter gangue particles, overflows at the lower drum end and is collected separately.

The key operational parameters that affect the MGS performance are drum rotational speed—governs applied g-force and particle migration rate; shaking frequency and amplitude—influence bed stratification and separation sharpness; drum inclination angle—impacts slurry residence time and film behavior; wash water flow rate—modulates film renewal and the rejection of lighter phases; and feed rate and pulp density—determine separation efficiency and throughput.

The MGS provides a highly effective and scalable solution for beneficiating fine and ultrafine mineral fractions by combining multiple acceleration vectors within a thin-film stratification environment. Its application is particularly advantageous in treating finely disseminated lateritic ores, where the traditional separation of gravity fails to achieve adequate recovery, especially for critical metals such as cobalt and nickel.

Table 1 presents the operational boundaries for the MGS during bench-scale experimentation. The system accommodates feed particles within a 500 to 1 μm range and supports a pulp solids concentration between 10% and 50%. Its throughput capacity varies from 10 to 25 kg/h. The drum operates at rotational speeds ranging from 100 to 300 rpm, critical for enhancing the separation process. A constant shaking amplitude of 10 mm is applied to facilitate the stratification of particles. The tilt angle (θ) can be adjusted from

0° to 9°, affecting the trajectory of the material on the drum surface. Additionally, wash water flow is regulated between 0 and 10 L/min to assist in the separation of finer particles and improve product quality.

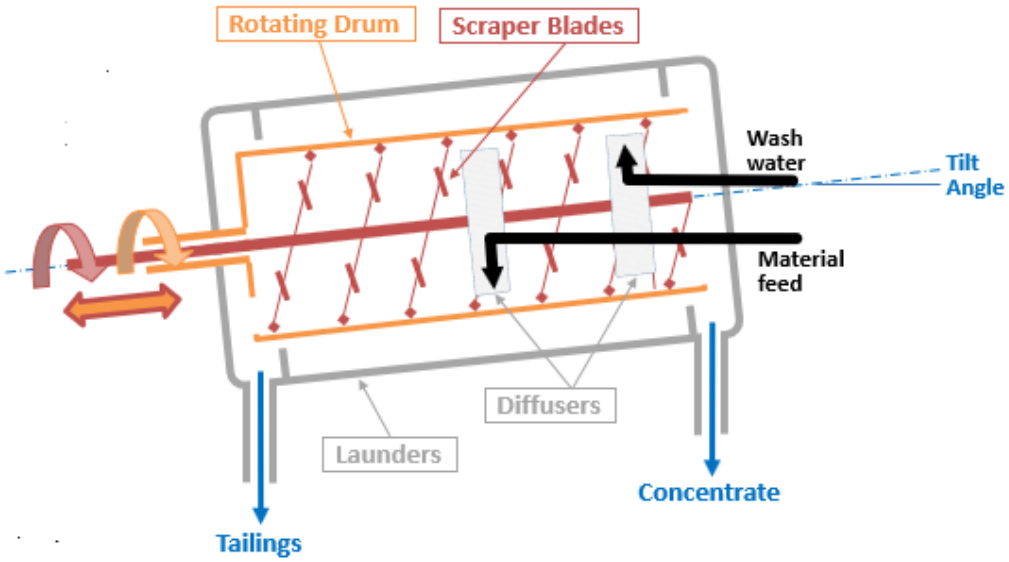

Figure 1. Multi-Gravity Separator. Source: Gravity Mining Ltd. (Cornwall, UK, 2025) [30].

Table 1. Operational limits to MGS in bench tests (Gravity Mining Ltd., 2025) [30–33].

MGS Operation Limits	
Feed particle size range, μm	500–1
Feed solid in pulp, %	10–50
Capacity, kg/h	10–25
Drum rotation speed, rpm	100–300
Shake amplitude, mm	10
Tilt angle, θ	0–9
Wash water, L/min	0–10

2.2. Methods

The experimental procedure evaluates the separation performance of lateritic ore from the Agios Ioannis deposit, a bulk mass. The process flow included sample preparation, comminution, particle size classification, and analytical testing, with subsequent homogenization and quartering to reproduce 14 aliquots. The flowchart in Figure 2 details the step-by-step process applied to the development of this investigation.

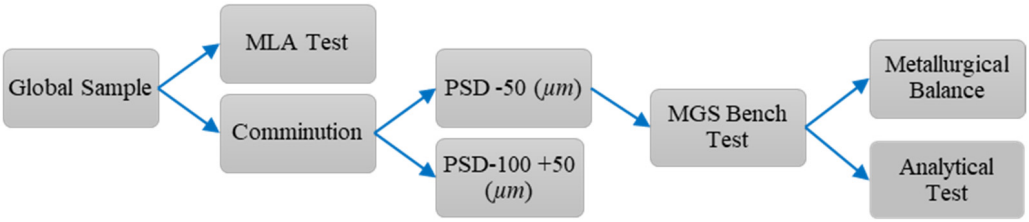

Figure 2. A flow chart that illustrates the process of sample preparation, physical separation, and analysis in the laboratory. A flow chart illustrates the process of sample preparation and physical separation. A flow chart demonstrates the laboratory's sample preparation process, physical separation, and analysis.

Initially, an aliquot was subjected to Mineral Liberation Analysis (MLA) to determine the mineralogical composition, particle size, mineral liberation characteristics, and their associations. The tests were carried out at the Laboratory John de Laeter Centre, Curtin University (Perth), on an MLA650 (FEI, Hillsboro, OR, USA) environmental scanning electron microscope equipped with a Bruker Quantax Esprit 1.9 EDS system with two XFlash 5030 SDD detectors (Bruker, Berlin, Germany), and the Brand and software package v3.1 was used.

On the other hand, the global mass (top size: −2 mm) was comminuted in an open circuit using two mills. The first was a roller mill, with 71.2 rpm, which produced a reduction ratio of 6:1 that was divided in two crushing stages, in the second grinding, the global mass had a reduction ratio of 3:1, where the under size will pick up to −0.1 mm, and was submitted to a rod mill, with 71 rpm.

After milling, representative masses were generated, one in the fraction −100 +50 µm and another under 50 µm. These masses were reproduced in 7 aliquots for each fractions, both intended for testing in an MGS, with a methodology aligned with the design of experiments in Section 2.1.

The MGS bench tests were carried out with the following operational variables: drum speed, inclination angle, and wash water flow rate, with other fixed parameters, both detailed in Section 2.1. After the bench tests, the particle size distribution of the feed, concentration, and rejects was performed using a laser diffraction particle sizer.

Also, the resulting masses consisted of concentrates and rejects. These masses were dried at a temperature of 80 °C for 24 h for subsequent evaluation of contents by X-ray Fluorescence (XRF) with a Malvern Panalytical system, model Epsilon 1.

The XRF data reproduced in oxide form were processed and plotted in a mass balance for each test, followed by the cut distribution, metallurgical recovery, and asbolane mineral recovery in the concentrate.

2.3. Experimental Design

Three factors and three levels (kn-p) were considered for the design of experiments, planned in the MiniTab 19 software. The fractional experimental design was developed using a systematic approach to evaluate the operational parameters with the greatest significant effect. The parameters were categorized into three distinct levels: low (−1), medium (0), and high (+1), as described in Table 2. This structured design allows for the investigation of the linear and non-linear effects of the variables on the response metrics, providing a comprehensive understanding of their influence on the process as a whole.

Table 2. Parameters are categorized into bench tests.

Parameters	Symbol	Low	Middle	High
		−1	**0**	**+1**
Drum speed (*r*), rpm	x_1	170	260	330
Tilt angle (θ), °	x_2	4	6	8
Wash water rate, (*w*), L/min	x_3	0.5	1	1.5
Shake frequency (*sf*), spm	x_4	374	374	374
Feed solid rate (*fs*), %	x_5	30	30	30
Stroke amplitude, (*sa*), mm	x_6	10	10	10
Pulp feed rate (*pf*), lpm	x_7	~0.5	~0.5	~0.5

The operating parameters were considered according to the manufacturer's recommendation, whose understanding of the parameters includes:

1. Drum speed (r): Controls centrifugal force and particle retention time, where higher speeds improve separation of finer, denser particles but can reduce recovery if excessive. The drum speed range was 170 to 330 rpm, covering typical industrial operating conditions.
2. Tilt angle (θ): Affects the flow velocity, material flow, and stratification. Inclination angles between 4° and 8° are commonly used in gravity separators, between productivity and separation efficiency.
3. Wash water rate (w): Influences particle washing and the removal of fine and light particles. The water flow rate, pre-established as having the most significant effect, is between 0.5 and 1.5 L/min, aiming to evaluate the impact on improving concentrate quality.
4. Shake frequency (sf): This parameter influences the shear force generated by the back-and-forth oscillation, enhancing the movement of higher-density particles while impeding that of lower-density ones. Its effectiveness is also supported by fluid dynamics and the system's inclination. The frequency was set at 374 strokes per minute (spm), a value determined through preliminary experiments that showed it provided stable and efficient particle separation.
5. Feed solids rate (fs): Based on preliminary trials, the feed solids rate was fixed at 30%, which indicated that this concentration provided stable suspension viscosity and reliable flow behavior. Maintaining this constant ensured consistency across tests and minimized variability due to changes in rheological properties.
6. Stroke amplitude (sa): Regulates the agitation of the fluidized bed and the migration of dense particles in the direction opposite to the inclination of the drum. The manufacturer limits this parameter. The manufacturer limits this parameter in the equipment used in the tests, and its value is 10 mm.
7. Pulp feed rate (pf): Kept constant at 0.5 L/min to avoid confounding effects caused by fluctuations in flow rate.

Experimental levels [27,34] were selected as low–medium–high ranges based on:

- Literature benchmarks for similar separation systems.
- Pilot tests indicating thresholds for effective operation.
- Industrial relevance, ensuring the practical applicability of results.

The modeling of these experiments is assisted by the response surface methodology (RSM) or factor analysis, allowing process optimization while controlling noise variables. This approach facilitates the identification of optimal operating conditions through the statistical evaluation of the effects of the parameters.

The three-level experimental design, with variables coded (−1, 0, +1), was used to analyze the synergism between effects. As illustrated in Table 3, this experimental structure is based on the design of experiments (DOE) methodology, which of the main and interaction effects in multiple factors.

The independent variables were identified with symbols (x_1, x_2, and x_3) and are drum speed (x_1), number of revolutions per minute (rpm), theta tilt angle (x_2), adjusted in degrees (°), and wash water flow rate (x_3). The variables identified from x_4 to x_7, already detailed previously, were kept constant.

Each factor was categorized into three levels: low (−1), medium (0), and high (+1). These values are summarized in Table 3 to normalize the data of the lower, intermediate, and higher levels, used to facilitate the construction of polynomial regression models for subsequent statistical analysis.

Table 3. Coded levels with the experimental design.

Parameters	Symbol	Low	Middle	High
Drum speed (*r*), rpm	x_1	−1	0	+1
Tilt angle (a), θ°	x_2	−1	0	+1
Wash water rate, (w), L/min	x_3	−1	0	+1

Using the experimental data, the results are subjected to analysis of variance (ANOVA) to determine the statistical significance of each factor and the effects of their interactions. ANOVA quantifies response, each independent variable's contribution to the response's overall variation, thus allowing the identification of the parameters with the greatest synergism. This structured experimental plan of the hierarchical influence of the combination of operational parameters, best drum inclination angle, best rotation speed, and best wash water flow rate to maximize separation performance.

To quantify the MGS operational variables that reproduce the most significant response effect in the recovery of asbolane ore, the software mentioned above determines the main effects by calculating the weighted average derived from the analysis of variance (ANOVA) that decomposes the total variation in the response into individual contributions of the factors and interactions, using Equation (1).

$$R_E = \frac{1}{n}\sum_{i=1}^{n}(x_i : y_i) \quad (1)$$

where

R_E: mean of the response effect;
x_i: value of the factor for each *i*-th trial;
y_i: value delivered for the *i*-th trial;
n: total observations;
Σ: sum of $x_i \cdot y_i$ for all i.

3. Results and Discussion

3.1. MLA Results: Liberation Characteristics of Asbolane

Figure 3 shows a 3D class content distribution plot illustrating the liberation behavior of asbolane, represented as $Ni_4Co_{1.3}Ca_{0.1}Mn_{1.5}O_{10}-5(OH)_2-0.6H_2O$, across three particle size fractions: $Ni_4Co_{1.3}Ca_{0.1}Mn_{1.5}O_{10}-5(OH)_2-0.6H_2O$: 0–100 μm, 400–500 μm, and 900–1000 μm. The *x*-axis corresponds to the grade class, defined as the proportion of asbolane present in individual particles, segmented into ten intervals ranging from 0% to 10% (least liberated) to 100% (fully liberated). The *y*-axis indicates the weight percentage (wt.%) of particles falling into each grade class, and the *z*-axis reflects the particle size range (μm).

Fully liberated particles—those falling into the 90%–99% and 100% grade classes—are more amenable to efficient recovery by physical separation techniques. The distribution for the fine size fraction (0–100 μm) shows a dominant presence in these high-grade classes, indicating a high degree of liberation and favorable separation potential. In contrast, the coarser fractions, particularly the 900–1000 μm range, show a significant proportion of particles in the lower grade classes (e.g., 0%–10%, 10%–20%), indicating a predominance of composite particles where asbolane is insufficiently liberated from the gangue matrix.

These results highlight the inverse relationship between particle size and liberation: finer particles tend to be more liberated, while coarse particles often encapsulate asbolane in gangue, reducing recovery efficiency. This distribution therefore informs critical decisions

regarding comminution strategies, suggesting that further grinding may be required to increase liberation in coarser size fractions and improve overall process performance.

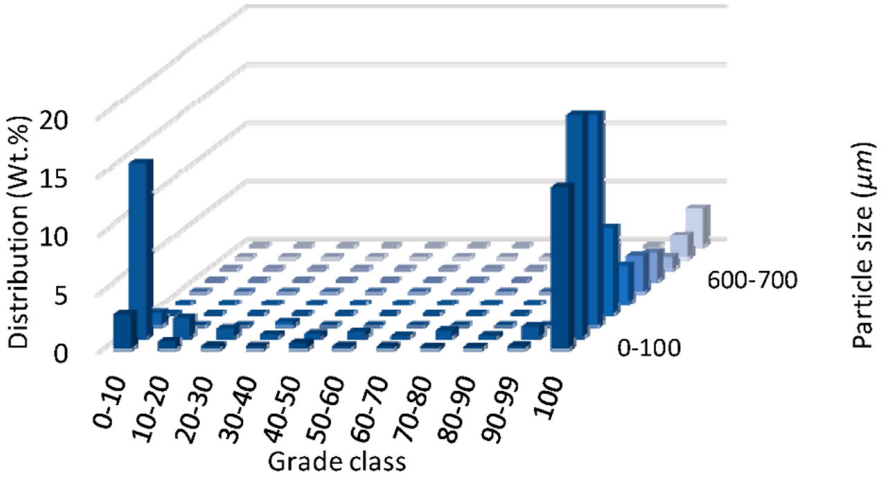

Figure 3. Class-grade liberation of particles from Agios Ioannis laterite, where asbolane is liberated.

The mineralogical analysis using MLA software (v3.1) identified the target phase as asbolane, with an empirical composition of $Ni_{0.3}Co_{0.3}Ca_{0.1}Mn_{1.3}O_{1.5}(OH)_2 \cdot 0.6H_2O$. Confirming this complex manganese–cobalt–nickel oxide structure through reference library matching provides significant insights into its liberation characteristics during comminution and classification processes. It is imperative to comprehend the liberation behavior of asbolane, as it significantly influences the efficiency of downstream recovery methodologies.

The 3D class-content distribution analysis (Figure 3) shows that asbolane is mainly associated with fine particles, especially in the 0–100 μm range, where it often appears nearly fully liberated (>90% liberation). This suggests effective mineral release due to fine grinding, which exposes grain boundaries and breaks down intergrowths, aiding separation during beneficiation.

However, high liberation is not limited to fine sizes. Notably, a significant portion of liberated asbolane is also found in larger size ranges: about 8% in −400 + 300 μm, 18% in −300 + 200 μm, 19% in −200 + 100 μm, and 14% in <100 μm. This indicates efficient liberation can occur without excessive grinding, likely due to favorable ore textures or natural breakage paths.

These results reflect a complex texture, with asbolane occurring as fine liberated grains and inclusions within coarser particles. This dual occurrence highlights the need for tailored crushing and separation strategies.

Mineralogical data [7] show that asbolane is associated with Fe oxides/hydroxides and vermiculite, supporting a supergene origin linked to intense lateritic weathering. Fe oxides incorporate Co, Ni, and Mn via substitution, while vermiculite offers interlayer spaces for metal retention. Minor quartz and chlorite may reflect original rock or early alteration residues.

Despite good liberation in fine sizes, asbolane often lacks exposed surfaces, indicating encapsulation. This can limit recovery using conventional methods due to processing challenges with ultrafines. Therefore, improved grinding methods and advanced separation techniques, like multi-gravity separation, are recommended to enhance recovery. These insights highlight the importance of detailed mineralogical studies for optimizing the processing of Co- and Ni-rich laterites.

3.2. Results of Experimental Design MGS Test (−100 +50 µm)

Table 4 presents a series of experimental results of the MGS tests (t_1 to t_7) for particle size fraction −100 +50 µm, evaluating the efficiency of a mineral concentration process gravity separator. The variables studied are: X_1: inclination angle (θ); X_2: drum speed (CMP); X_3: wash water flow rate (L/min). Showing the effects of tilt angle (θ), drum speed (CMP), and wash water rate, the measured responses include mass recovery and asbolane recovery (cobalt/nickel/manganese mineral).

Table 4. Results of experimental design MGS test in −100 +50 (µm) range.

Test Work	Tilt Angle, θ	Drum Speed, rpm	Wash Water Rate, L/min	Feed, g	Mass Recovery, %	Concentrate Mass, g	Tailings Mass, g	Asbolane Recovery, %	R_E, % $R_E = \frac{1}{n}\sum_{i=1}^{n}(x_i{:}y_i)$
	x_1	x_2	x_3						
t_1	−1	0	−1	195.4	0	0	195.4	0	0
t_2	0	0	−1	165.4	62.85	103.95	61.45	47.7	14.1
t_3	1	0	−1	176.45	80.99	142.9	33.55	53.9	98.2
t_4	1	−1	−1	178.3	81.3	144.95	33.35	76.8	100
t_5	1	1	−1	176.9	79.9	141.35	35.55	66.0	68.5
t_6	1	1	0	123.45	27.18	33.55	74.5	65.3	36.7
t_7	1	1	1	109.95	36.74	40.4	67.6	35.1	8.9

The recovery of asbolane ore subjected to the combined effects of the three operational variables revealed the following analysis:

Effect of drum tilt angle (x_1). The tilt angle demonstrated the most significant influence on mass and asbolane recovery among the factors studied. Tests conducted with high tilt angles (+1), notably in t_3, t_4, and t_5, achieved the highest recoveries of asbolane ore, with values ranging from ~66 to 76.8 (%). The most optimized response effect (RE) was reproduced in test t_4, reaching 100%, resulting in a ~76.8% recovery of the mass of asbolane ore.

Effect of drum speed (x_2). The rotation speed of the drum has a strong kinetic influence, modifying the separation dynamics, kinetic energy, and shear zone in the separation cut. Higher drum speeds recorded in tests t_4 (−1) and t_5 (+1) resulted in marginal improvements in the mass recovery of asbolane ore and concentrate mass. Although the effect was secondary to the tilt angle, it is hypothesized that the increased rotational movement induced turbulence, thus aiding in the release of fine particles while preventing their entrapment in the reject flow. However, it is essential to note that excessively high speeds can lead to mechanical carryover or particle detachment, highlighting the need for careful control.

Effect of washing water rate (x_3). In contrast to prevailing assumptions in wet separation systems, an increase in the washing water rate reflects a dilution behavior opposite to stratification. Its effect resulted in a reduction in the recovery of asbolane ore. The tests with the least impact, t_6 and t_7, involved moderate to high washing water flows (x_3 = 0 or +1), resulting in 36% and 8.9% response effects. These values are contrary to the mass recovery of asbolane ore, as their mass recovery of the mineral was 65% and 35%, respectively.

The factorial design reveals significant interaction effects among the variables. For instance, while a high tilt angle alone improved recovery, its impact was nullified at high water flow, as evident in test t_7 (asbolane recovery: 35.10%; response effect: 8.90%). Furthermore, test t_1, operated with all parameters at minimum levels, exhibited complete process failure (0% recovery), thereby underscoring the necessity for a minimum threshold of kinetic and gravitational forces to initiate separation.

The center point (t_2) yielded moderate recovery values, suggesting non-linear relationships and possible curvature in the response surface. This finding validates the implementation of response surface methodology (RSM) or second-order regression models for further process optimization.

3.3. Results of Experimental Design MGS Test (−50 µm)

The experiments conducted with −50 µm fraction aliquots are described in Table 5, which shows the results of a series of test experiments (t_1 to t_7) carried out under the same operational conditions mentioned in the section above.

Table 5. Results of experimental design MGS test (−50 µm).

Test Work	Drum Speed, CMP	Tilt Angle, θ	Wash Water Rate, L/min	Feed, g	Mass Recovery, %	Concentrate Mass, g	Tailings Mass, g	Asbolane Recovery, %	Response Effect, %
	x_1	x_2	x_3						
t_1	0	−1	−1	168.1	0.0	0.0	168.05	0.00	0.0
t_2	0	0	−1	167.15	4.58	7.65	159.5	55.60	67.2
t_3	0	+1	−1	177.2	32.05	56.8	120.4	65.80	79.6
t_4	−1	+1	−1	177.75	32.69	58.1	119.65	77.80	94.1
t_5	+1	+1	−1	177.85	22.41	39.85	138	82.70	100.0
t_6	−1	+1	0	160.15	12.02	19.25	140.9	78.00	94.3
t_7	−1	+1	+1	149.73	2.89	4.327	145.4	43.00	52.0

Influence of tilt angle (x_2). A clear trend emerges regarding the tilt angle. The data show a substantial increase in both mass recovery (0.0% to 4.58% to 32.05%) and asbolane recovery (0.0% to 55.60% to 65.80%) when the tilt angle was increased from a low angle (−1 in t_1) to a medium (0 in t_2) and then to a high angle (+1 in t_3), while keeping all other parameters constant. This finding indicates that increasing the tilt angle facilitates the transport and collection of the asbolane-rich fraction, likely by influencing the gravitational forces acting on the particles and the slurry flow dynamics within the MGS apparatus.

Effect of drum speed (x_1). The impact of drum speed becomes more apparent when comparing experiments with a high tilt angle and low wash water rate (t_4 and t_5). A slower drum speed (−1 in t_4) yielded slightly higher mass recovery (32.69%) and asbolane recovery (77.80%) compared to a faster drum speed (+1 in t_5, with 22.41% and 82.70%, respectively). However, the highest overall response effect was observed at the faster drum speed (t_5). This finding suggests a possible trade-off: while a slower speed may result in a greater quantity of recovered material, a quicker speed, under these specific conditions, may yield a higher quality concentrate, as reflected by the optimized response effect.

The role of wash water rate (x_3) was investigated, and the results significantly influenced the separation process. A comparison of experiments t_4, t_6, and t_7 (all with a high tilt angle and a slower drum speed) revealed a non-linear relationship with recovery when the wash water rate was varied from low (−1 in t_4) to medium (0 in t_6) and then high (+1 in t_7). A medium wash water rate (t_6) resulted in a lower mass recovery (12%). Still, it maintained a high asbolane recovery (78%), suggesting it might effectively wash away unwanted material while retaining the valuable asbolane. Conversely, an elevated wash water rate (t_7) resulted in a substantial decline in both mass recovery (2.89%) and asbolane recovery (43%), signifying that excessive washing may lead to the loss of valuable fine particles.

Interaction of variables and optimization. The highest response effect achieved in experiment t_5 (drum speed +1, tilt angle +1, wash water rate −1) highlights the importance of considering the synergistic effects of the operating variables. This specific combination of parameters is the most effective among those tested for achieving the desired separation outcome, as defined by the response effect. Further investigation into these conditions, with finer adjustments to the drum speed, could lead to even greater optimization.

This experimental study demonstrates that the recovery of fine asbolane particles using the MGS test is significantly influenced by the drum speed, tilt angle, and wash water rate. The tilt angle emerges as a pivotal factor in achieving initial recovery. At the same time, the drum speed and wash water rate play crucial roles in balancing the quantity and potentially the quality (purity) of the recovered concentrate. The optimal conditions identified in this study (as indicated by the highest response effect) provide a valuable starting point for further process optimization.

3.4. Experimental Design Results: Interpretation of the Effect of the Responses

3.4.1. Size Range −100 +50 µm

Figure 4 illustrates the main effects on mass recovery for the −100 +50 µm size fraction. The figure presents three distinct curves, each representing the influence of one independent variable (x_1, x_2, x_3) on the recovery of asbolane. To analyze and visualize these effects, a Python program (Python 3.x) was used to process the data and generate the corresponding plots, allowing for a clear comparison of how each variable influences asbolane recovery. Vertical axis: adjusted mean asbolane recovery.

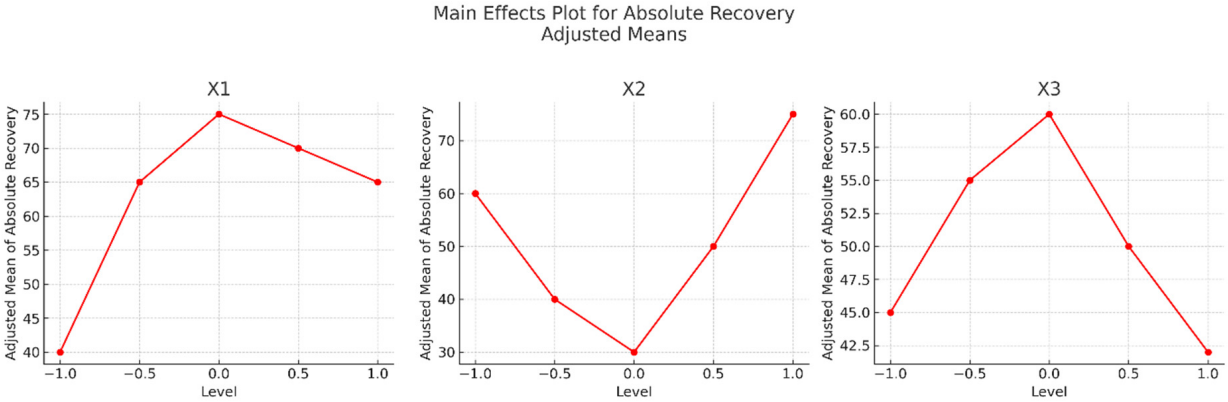

Figure 4. Main effects plot for mass recovery.

Horizontal axis: factor levels (typically −1 and +1 for factorial studies).

- x_1: The curve for x_1 shows significant fluctuations. At −1, recovery is high, while it decreases at +1. This suggests that variable X_1 hurts asbolane recovery as its level increases.
- x_2: While the curve for x_2 shows significant fluctuations, at −1, recovery is high at +1. This suggests that increasing variable X_2 has a positive effect on asbolane recovery.
- x_3: The curve for x_3 shows a similar trend to x_1, with recovery higher at −1 and a decrease at +1. This also indicates that increasing x_3 hurts asbolane recovery.

The data indicate that the tilt angle (θ), drum speed, and wash water rate significantly affect recovery outcomes. Notably, the maximum absolute recovery (100%) was attained at a tilt angle of +1, a drum speed of −1, and a wash water rate of −1, thereby underscoring the significance of parameter synergy. Conversely, an increase in drum speed to +1 under the same tilt angle (+1) reduced absolute recovery to 65.3%, underscoring a pronounced interaction effect between these variables.

Table 3 presents the experimental design of the MGS tests within the particle size range of −100 to +50 µm; significant variability was observed in mass recovery outcomes. Test 1 exhibited an anomalously high mass recovery (195.4 g) yet yielded zero absolute recovery, indicating ineffective retention of the target material despite substantial throughput. In contrast, test 4—conducted with drum rotation and tilt angle parameters set to −1 and +1, respectively—demonstrated optimal performance, achieving a mass recovery of 178.30% and an absolute recovery of 76.80%. Furthermore, the data reveal an inverse correlation between water flow rate and absolute recovery, suggesting that lower water rates enhance the selective retention of the target material, particularly when combined with favorable tilt settings.

The response effect metric, which peaks at 100% under optimal conditions, validates the parameter combinations necessary for efficient recovery. However, a sharp decline in performance at extreme drum speed (+1) and water rate (+1) settings is indicative of operational limits. This behavior suggests that process efficiency is highly sensitive to parameter balance, with tilt angle as a pivotal factor.

Implementing a tilt angle of +1, in conjunction with the reduction in drum speed and water rates, optimizes absolute recovery.

Figure 5 analyzes the combined effect of tilt angle and drum speed on asbolane recovery, measured via adjusted Y-concentrate averages. The figure highlights that the efficiency of the Multi-Gravity Separator depends on the balance between the inclination angle and the drum speed. A strong interaction shows that these parameters are optimized independently, but in tandem. Tilt angle and drum speed are the two parameters studied, each tested at three coded levels (−1, 0, 1). These levels represent low, medium, and high settings, particularly for coarse particles in the −100 +50 µm fraction.

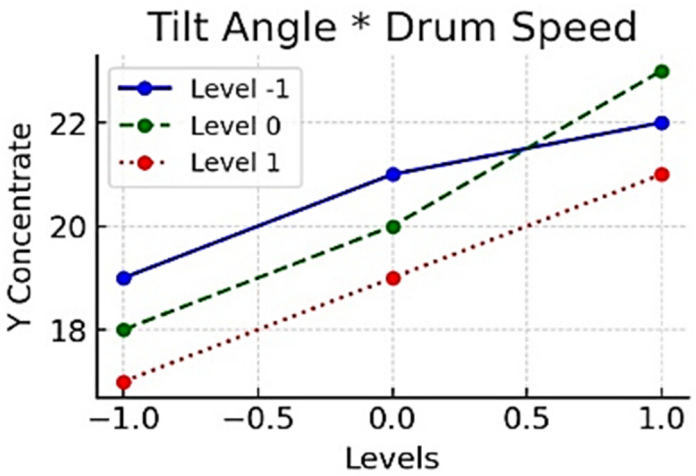

Figure 5. Interaction plot for the adjusted means of concentrate Y (asbolane recovery −100 +50 µm).

The interaction between tilt angle and drum speed plays a crucial role in asbolane recovery, as demonstrated by Figure 5 and supporting experimental data summarized in Table 2. Recovery generally increases with drum speed across all tilt angle levels; however, the magnitude of this effect is strongly dependent on the tilt angle. At a Level 1 tilt angle, recovery performance is consistently superior across the tested drum speed range. This is evidenced by test t_5, which recorded the highest asbolane recovery of 76.50%, coinciding with a moderate drum speed (Level 0). Although this test also shows an anomalously high mass recovery (144.95%), likely due to sample retention or measurement artifacts, the recovery trend remains valid. In contrast, test t_6 (tilt +1, speed +1) exhibits a significantly lower recovery of 53.10%, suggesting that excessively high tilt angles may disrupt flow stability or reduce residence time, adversely affecting coarse particle separation.

The interaction plots further reveal a moderate synergistic effect between the two variables. While all curves show a positive trend with increasing drum speed, the slope is steepest under Level 1 tilt conditions, indicating that the positive impact of drum speed is maximized when the system operates at a reduced inclination. This pattern supports that mechanical stability at low tilt angles enhances particle capture, especially in gravity-driven separation processes such as the Multi-Gravity Separator (MGS).

Additionally, supporting metrics from Table 2, such as concentrate grade and tailings mass, reinforce this conclusion. Tests t_3 and t_5, both conducted at Level −1 tilt, not only deliver high recoveries (+73%) but also maintain relatively low tailings mass percentages (~33 to 35%) and favorable concentrate grades (>30%). This confirms that mechanical configuration is critical in effectively separating coarser particles, likely due to minimized turbulence and controlled settling environments.

The findings underscore the importance of optimizing tilt angle with drum speed to achieve high recovery in coarse fractions. Specifically, low tilt angles combined with moderate-to-high drum speeds yield optimal results for the −100 +50 µm size class. The mechanical behavior of larger particles necessitates stable flow conditions, where excessive inclination may cause adverse flow regimes, such as short-circuiting or increased back-mixing.

These outcomes are consistent with previous research on gravity-based separation, which emphasized the importance of controlling residence time and flow stability to ensure effective separation efficiency. It is recommended that future investigations incorporate computational fluid dynamics (CFD) modeling to quantify flow behavior under varying tilt-drum settings.

3.4.2. Size Range −50 µm

Figure 6 illustrates the main effects plot for mass recovery in the −50 µm particle size fraction, supported by the experimental results in Table 3. The three factors investigated, tilt angle (x_1), drum speed (x_2), and wash water rate (x_3), demonstrate varying degrees of influence on mass recovery, with wash water rate (x_3) emerging as the most significant factor.

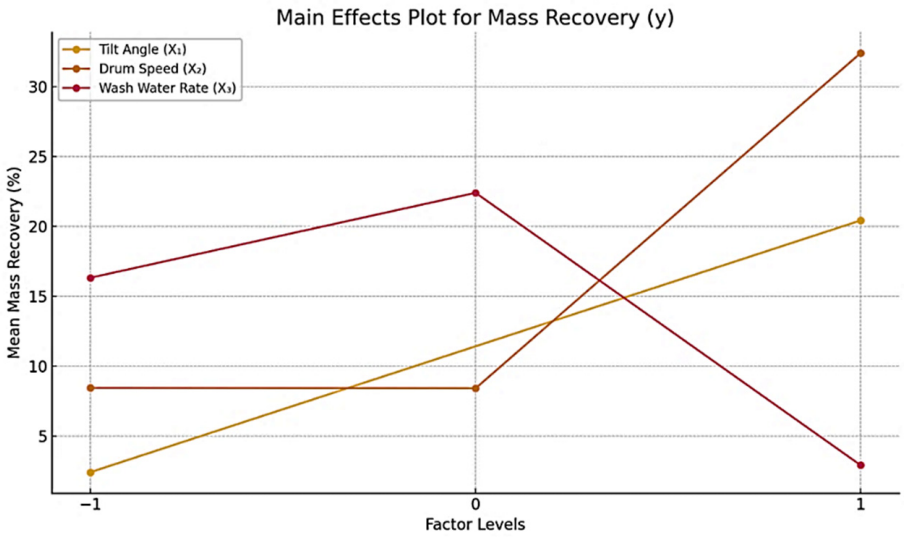

Figure 6. Main effects plot for mass recovery −50 µm.

The steep slope of the wash water rate curve in Figure 6 indicates a substantial negative effect on mass recovery as the factor level increases from −1 to +1. Based on the results shown in the table, this inverse relationship suggests that higher wash water rates lead

to reduced mass recovery, likely due to excessive turbulence and enhanced entrainment of fine particles into the tailings stream. This trend is consistent with the lowest mass recovery value (2.89%) observed in test t_7, which coincides with the highest wash water rate (+1) and further confirms the destabilizing effect of excessive wash water in ultrafine particle separation.

In contrast, the drum speed (X_2) shows a positive linear trend, where increasing drum speed enhances mass recovery. This may be attributed to improved stratification and residence time, which facilitate the separation of fine particles. The trend is reflected in tests t_3 and t_4, where a combination of high drum speed and low wash water rate yields mass recoveries exceeding 30%.

The tilt angle (X_1) has a comparatively moderate but meaningful effect, with a slightly increasing trend toward higher factor levels. Its influence appears to be less pronounced in this acceptable size range, possibly because finer particles are more responsive to hydrodynamic forces than tilting gravitational components.

The maximum mass recovery of 32.69% is achieved in test t_4 (tilt −1, speed +1, wash −1), which corresponds to the optimal configuration in terms of reduced wash water and increased drum speed; this test also yielded one of the highest asbolane recoveries (77.80%), reinforcing the idea that controlled wash water and sufficient mechanical agitation are critical for optimizing fine particle recovery.

The response effect values further validate the trends observed in the main effects plot. The most significant response (100.0) is associated with test t_5, which combines a high drum speed with low wash water rate and moderate tilt angle, demonstrating the synergistic effects of mechanical and hydrodynamic controls.

Figure 7 shows the interaction plot for the adjusted means of concentrate Y (asbolane recovery), −50 μm. Interaction plot showing the adjusted means of concentrate Y (asbolane recovery) for different factor combinations: drum tilt × rotation speed, drum tilt × wash water flow rate, rotation speed × wash water flow rate. The curves correspond to the different levels of the coded factors (−1, 0, +1).

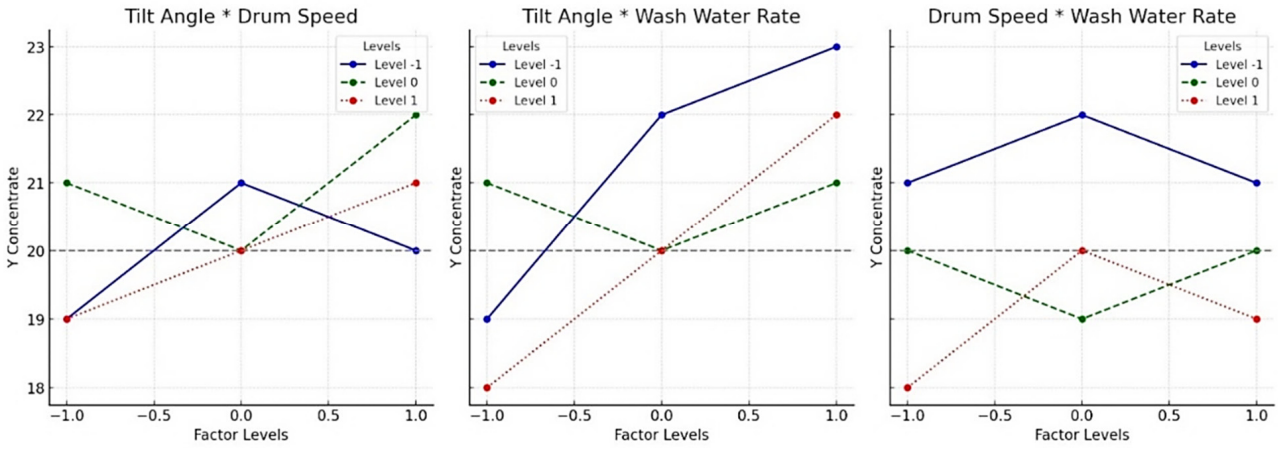

Figure 7. An interaction plot for the adjusted means of concentrate Y (asbolane recovery), −50 μm.

Factor interaction analysis reveals notable combined effects on asbolane recovery. Three factors were evaluated to detect potential synergies or antagonisms on influencing the response variable (Y).

Drum tilt versus rotation speed. A moderate interaction is observed. The curves are not parallel, indicating that the effect of rotation speed varies depending on the tilt. More specifically, a high inclination improves recovery. Conversely, when the speed is low, the inclination is less pronounced, or even the opposite is less pronounced.

Drum inclination versus wash water flow rate. This interaction is the most pronounced of the three studied. The lines intersect, suggesting a strong dependence between the two factors. The inclination effect remains present at low water flow rates. Still, it is significantly amplified as the water flow rate increases. This suggests that process efficiency is particularly sensitive to joint optimization of these two parameters.

Rotation speed versus wash water flow rate. A weak interaction is noted. The lines are nearly parallel, indicating the independence of the respective effects of speed and water flow rate. Each factor can therefore be adjusted separately without altering the effect of the other.

The interaction curves for asbolane recovery reveal distinct optimization strategies based on particle size. In the −100 +50 (µm) fraction, factors like drum inversion (reverse mode) and extended processing time (120 min) enhance recovery by ensuring mechanical stability for coarse particles. In contrast, the finer fraction appears to have a higher recovery −50 µm fraction is highly influenced by hydrodynamic factors such as wash water flow rate, turbulence (controlled by drum inclination), and flow regime stability. These factors explain the 82.2% recovery plateau in fine particles (based on combinations of variables shown in Table 4), emphasizing processing challenges.

3.5. Mass Balance

3.5.1. Size Range −100 +50 µm

Table 6 presents them as a balance of the size fraction −100 +50 µm. According to the MLA results, the analyzed data emphasized the elements Mn, Co, and Ni, constituents of the liberated asbolane mineral. The contents of and the metallurgical recovery of these elements are noted for each test in Table 6 with mass recovery (mR), respecting the criteria of the experimental model of Tests 1 to 7.

Table 6. The mass balance of the size fraction −100 +50 µm.

Test	mR %	Content						Metallurgical Recovery					
		MnO		Co_3O_4		NiO		MnO		Co_3O_4		NiO	
		C %	W %	C %	W %	C %	W %	C%	W%	C %	W, %	C %	W %
1	0.0	0.00	0.60	0.00	0.34	0.00	1.51	0.0	100	0.0	100.0	0.0	100.0
2	62.8	0.60	0.75	0.40	0.30	1.29	1.90	57.4	42.6	69.5	30.5	53.5	46.5
3	81.0	0.61	0.73	0.36	0.31	1.49	1.92	78.0	22.0	83.1	16.9	76.7	23.3
4	81.3	0.62	0.74	0.38	0.32	1.50	1.94	78.3	21.7	83.4	16.6	77.1	22.9
5	79.9	0.62	0.74	0.37	0.32	1.53	1.93	76.7	23.3	82.4	17.6	75.9	24.1
6	78.6	0.60	0.76	0.39	0.32	1.43	1.96	74.3	25.7	81.6	18.4	72.8	27.2
7	73.1	0.57	0.73	0.41	0.32	1.35	1.91	68.1	31.9	77.8	22.2	65.7	34.3

C: concentrate. W: tailings.

The table demonstrates the effectiveness of the MGS process in recovering manganese (MnO), cobalt (Co_3-O_4), and nickel (NiO), while simultaneously minimizing tailings. The manganese recovery in the concentrate exhibited a substantial increase from 17.4% in test 2 to a maximum of 78.3% in test 4, underscoring the efficacy of optimizing MGS parameters. Concurrently, there was a decline in manganese losses to tailings, which decreased from 42.6% to 21.7% over the same period. However, beyond test 4, MnO recovery declined to 68.1% by test 7, potentially due to operational constraints (drum inclination × wash water flow rate). Cobalt demonstrated the highest recovery efficiency, reaching 83.4% in test 4, with consistent performance above 80% in tests 3 through 6 and minimal losses to tailings.

Nickel recovery exhibited a comparable trend to manganese, reaching a maximum of 77.1% in test 4 before gradually decreasing to 65.7% by test 7. The behavior of asbolane, a host mineral for Mn, Co, and Ni, aligned closely with the recovery patterns of these metals, suggesting effective liberation and separation. Test 4 represented optimal process performance, with recoveries for all three elements ranging from 77.1% to 83.4%. While earlier projections indicated 85%–90% recovery, the data shows slightly lower but still robust performance. The decline in recoveries observed in subsequent tests underscores the significance of process stability and feed consistency. The MGS process is valuable for enriching target metals, reducing tailings streams (with less than 23% of MnO, Co_3O_4, and NiO remaining in tailings during optimal operation), and enhancing cost-effectiveness.

The employment of density-based separation within the MGS framework ensures the attainment of high metallurgical recoveries (70%–83%) while concurrently fostering environmental sustainability. This approach is promising for the efficient processing of asbolane-bearing ores.

3.5.2. Size Range −50 μm

Table 7 shows the results of seven tests conducted under the same operational conditions as the previous tests in MGS. The values of metallurgical contents and mass balance were compared with the mass recovery (mR) for the elements MnO, Co_3O_4, and NiO in the asbolane ore.

Table 7. The mass balance of the size fraction −50 μm.

Test	mR, %	Content						Metallurgical Recovery					
		MnO		Co_3O_4		NiO		MnO		Co_3O_4		NiO	
		C %	W %	C %	W %	C %	W %	C %	W %	C %	W %	C %	W %
1	0	0.00	0.61	0.00	0.25	0.00	0.25	0.00	100	0.00	100	0.00	100
2	4.58	0.50	0.65	0.42	0.31	0.84	2.06	57	43	70	30	54	46
3	32.05	0.68	0.65	0.33	0.23	2.05	2.55	78	22	83	17	77	23
4	32.69	0.66	0.67	0.31	0.23	1.97	2.54	78	22	83	17	77	23
5	22.0	66.1	65%	35%	22%	1.77%	2.47	77	23	82	18	0.00	24
6	12.02	0.60	0.65	0.40	0.23	1.42	2.49	74	26	82	18	54	27
7	0	0.55	0.65	0.42	0.23	1.07	2.47	68	32	78	22	77	34

C: concentrate. W: tailings.

The concentration of different elements increases progressively, indicating efficient enrichment in MnO, Co_3O_4, and NiO, while the tailings decrease, confirming effective separation by the MGS. Metallurgical recoveries improve notably from Test 4, with MnO at 78% and Co_3O_4 at 77%, stabilizing around 77%–78% from Test 5 onward. Enrichment indices exceed 1.0 for MnO and Co_3O_4, highlighting effective mineral concentration and profitability. Oxide recovery follows a similar trend, peaking at 87% MnO and 52% Co_3O_4 in tests 5–6, reducing tailings losses. These results confirm the MGS's role in optimizing enrichment and recovery, with peak efficiency observed in tests 5–6, validating its benefit for profitable and sustainable asbolane mining.

MGS is more efficient on the −50 μm fraction with the coarser fraction, with better recovery and more marked enrichment in MnO and Co_3O_4. The −100 +50 μm fraction shows slightly lower performance, suggesting that treating finer particles optimizes recovery and process profitability.

3.6. Asbolane Mineral Concentration

3.6.1. Size Range −100 +50 µm

Figure 8 shows the distribution of NiO, Co_3O_4, and MnO in a sample with a particle size of −100 + 50 µm across seven test conditions (Test 1 to Test 7), with data reported for the feed (f), concentrate (c), and tailings (w). The vertical axis indicates oxide content (%), while the horizontal axis combines test numbers and corresponding feed content levels. Colored lines represent each oxide: green for NiO, orange for Co_3O_4, and blue for MnO. Within each color, different marker shapes distinguish the process stages (feed, concentrate, tailings). NiO exhibits the highest content in the feed, ranging from approximately 1.5% to 2.0%, and retains significant values in the concentrate phase, suggesting effective separation (e.g., 1.541% in test 6). Co_3O_4 and MnO display lower initial concentrations, with average values around 0.35%–0.45% and 0.6%–0.7%, respectively. Their moderate enrichment in the concentrate phase (e.g., 0.631% MnO, 0.363% Co_3O_4) indicates partial recovery. The figure highlights NiO's superior separation performance compared to the other oxides.

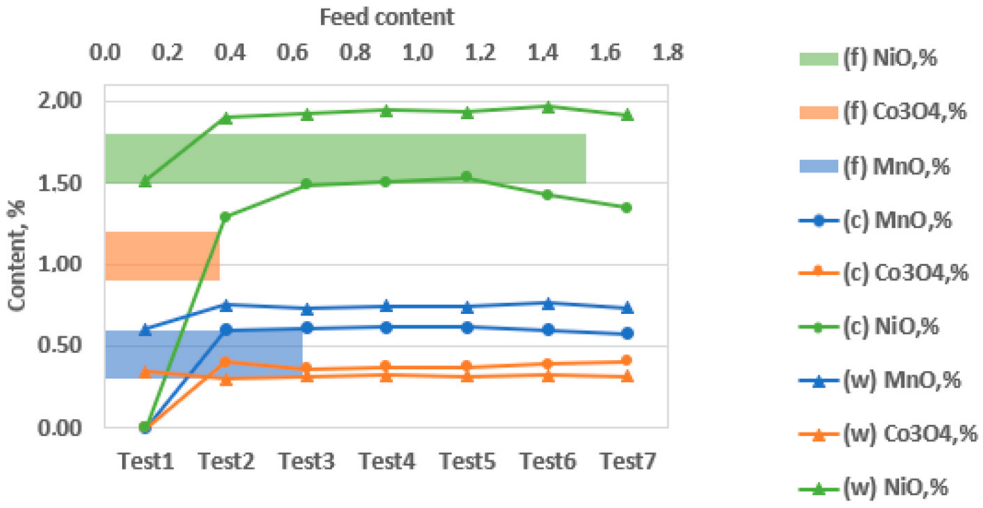

Figure 8. The distribution of oxides (NiO, Co_3O_4, MnO) in a sample with a particle size of −100 +50 µm. (f): feed (raw material before separation); (c): concentrate (enriched main product); (w): tailings.

The data demonstrates MGS's capacity to enrich valuable oxides while minimizing associated tailings. The synergy between key operational parameters, tilt angle, drum speed, and wash water flow plays a decisive role in this performance.

The experimental results from test 4 (x_1 = +1, x_2 = –1, x_3 = –1) reveal the optimal operating conditions for effective mineral separation. Under these settings, the process achieved the highest recovery rates, ranging from 77% to 83% for metal oxides and 76.8% for asbolane, while delivering significant enrichment and minimizing tailings. These findings underscore the importance of maintaining a precise operational window, as the separation efficiency is highly dependent on tightly controlled process parameters.

An analysis of the feed composition further supports these results, showing manganese oxide (MnO) as the most prevalent oxide at 1.541%, primarily due to the asbolane mineral present. Cobalt oxide (Co_3O_4) and nickel oxide (NiO) follow with concentrations of 0.631% and 0.363%, respectively. This composition highlights the challenges and opportunities for selective recovery of valuable metals in the feed material.

During concentration, all three oxides improved grades, with NiO displaying the most dramatic increase from 0.34% ($test_1$) to 1.50% ($test_4$), thanks to efficient density-based separation. Tailings levels drop accordingly, especially by test 4: MnO from 42.6% to 21.7%, Co_3O_4 from 30.5% to 16.6%, and NiO from 46.5% to 22.9%.

The performance of the MGS in terms of separation efficiency shows it is partially effective in concentrating metal oxides; however, missing data for key variables such as (c) and (w) limit a comprehensive quantitative assessment. Additionally, feed variability (*f*) poses challenges for reproducibility analysis. Among the critical parameters, the current particle size range of −100 +50 µm may not allow for complete mineral liberation, suggesting that finer grinding to below 50 µm could enhance separation efficiency. Additionally, particle size analysis focused on testing finer size ranges (−50 µm) to enhance mineral liberation and improve overall performance.

3.6.2. Size Range −50 µm

Figure 9 presents an analysis of the oxide composition of an asbolane mineral concentrate, with a reference mass of 50 µm. The oxides analyzed include NiO (nickel oxide), Co_3O_4 (cobalt oxide), and MnO (manganese oxide). The following results show the average of seven repeated tests. The *x*-axis (horizontal) of the graph indicates the various tests performed, numbered from $test_1$ to $test_7$, while the *y*-axis (vertical) represents the percentage content of metal oxides in the sample. Three metal oxides are analyzed: NiO (nickel oxide), Co_3O_4 (cobalt oxide), and MnO (manganese oxide). Additionally, three sample types are presented: (f) for feed (the raw material before separation); (c) for concentrate (the enriched main product); and (w) for rejects (tailings or residue).

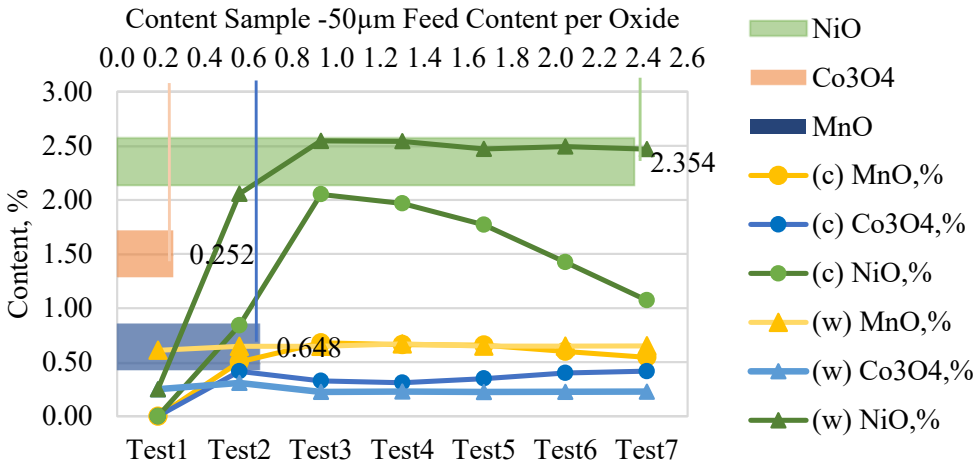

Figure 9. The distribution of metal oxides (NiO, Co_3O_4, MnO) in a sample with a particle size of −50 µm. (c): concentrate (enriched main product); (w): rejects (tailings or residue).

The specific values for each metal oxide in the concentrate are shown, with MnO at 2.35%, Co_3O_4 at 0.252%, and NiO at 0.65%. The colored curves in the graph illustrate the variation in the content of each metal oxide across the different tests.

The figure displays the material balance results after separating an asbolane concentrate rich in Ni, Co, and Mn using an MGS with a particle size of −50 µm. The feed (f) reflects the initial composition before separation, while the outputs include the concentrate (c), which is enriched in valuable metals, and the rejects (w), representing the depleted tailings. Seven tests were conducted, likely varying key operating parameters such as rotation speed, tilt angle, and water flow rate. The objectives include evaluating the separation efficiency of the oxides (NiO, Co_3O_4, MnO), quantifying the distribution of metals in the concentrate and reject fractions, and identifying optimization opportunities for the recovery of critical metals.

The MGS shows promising selectivity by partially enriching oxides in the concentrate, although residual losses are lost in the rejects. The lack of precise numerical values for the concentrate and rejects limits a quantitative assessment, but the notes suggest signif-

icant differences between the tests. Nickel (NiO) likely concentrates in the concentrate, while cobalt (Co_3O_4) and manganese (MnO) show a more complex distribution. The efficiency of the MGS varies between the tests, which could be due to adjustments to the device parameters.

For the separation of NiO (specific gravity ~6.6–7.4) from compounds such as Co_3O_4 (SG ~6.1) and MnO (SG ~5.2), gravity-based methods, including centrifugal concentrators and stabilizers, can be employed to exploit these specific gravity differences, achieving nickel recoveries of over 70% from laterites [27,28].

In tailings management, an economic threshold (w) for NiO/Co_3O_4 content can guide decision-making: reprocessing via flotation or acid extraction may be justified.

Typical nickel recovery from gravity-based processes ranges from 60 to 80. Research also shows that combination with other methods, recovery rates of above 80% are possible. Recovery rates of above 80% are possible when MGS is combined with different techniques. The recent result of the MGS recovery shows more than 80% recovery. Additionally, pilot-scale tailings reprocessing trials can be used to assess flotation performance at lower nickel and cobalt grades [34].

3.7. Metallurgical Recovery

3.7.1. Asbolane Mineral Concentrate Mass −100 +50 µm

Figure 10 presents the metallurgical recovery rates of asbolane, a cobalt-, nickel-, and manganese-rich mineral across seven Multi-Gravity Separator (MGS) tests, with the vertical axis representing recovery percentages and the horizontal axis denoting test numbers (1–7) with a particle size ranging between −100 and +50 µm.

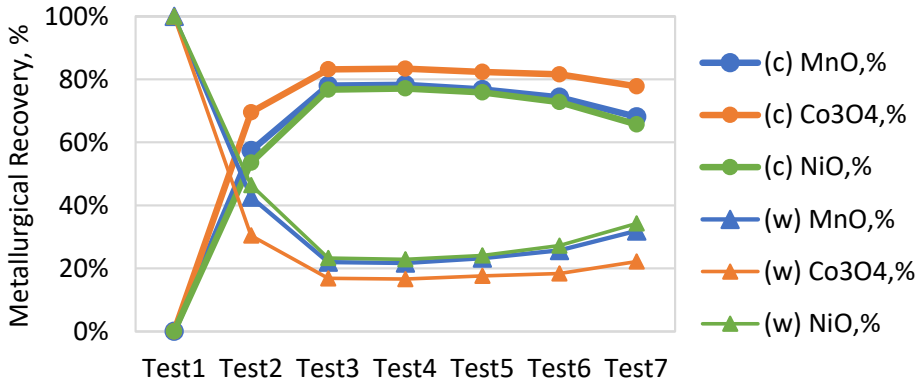

Figure 10. Asbolane mineral concentrate mass −100 +50 µm, where (c) is concentrate and (w) is residue (tailings).

Parameters such as tilt angle, drum speed, and wash water flow directly affect tilt angle, drum speed, and wash water flow. Operational parameters, as well as tilt angle, drum speed, and wash water flow, strongly influence recovery trends, directly affecting stratification and separation efficiency. Test 1, with a low tilt angle (–1), neutral drum speed (0), and low wash water (–1), yielded 0% recovery, demonstrating ineffective separation. In contrast, Test 4 (+1, −1, -11-1 1) achieved peak performance with 83.4% asbolane recovery and high-grade concentrates (MnO: 1.94%, Co_3O_4: 0.74%, NiO: 1.50%), highlighting the optimal parameter balance for maximizing retention and density-based separation.

Test 3, though showing the highest asbolane recovery (98.2%), produced lower metal oxide grades. Tests 5–7, characterized by high drum speeds and elevated wash water rates, saw declining recoveries (test 7: 35.1%) and increased metal losses. The variability in recovery (0%–100%) reflects the MGS's sensitivity to parameter shifts, where minor deviations can significantly affect recovery rates and concentrate quality. Importantly,

asbolane recovery correlates strongly with metal enrichment, reinforcing its role as a key carrier of Mn and Co.

This is to identify the optimal conditions (rotation speed, wash water flow rate, and inclination) for maximizing the recovery of metals (Mn, Co, Ni). However, the variability of results, with recoveries ranging from 0.0% to 100.0% (83.4% for test 4 and 0% for test 1), suggests that some tests are more effective than others in achieving this goal.

This sets the value of the efficiency of the MGS to concentrate the metals (Mn, Co, Ni) in the asbolane mine (100–50 µm). The results contain significant variations in the recovery rate (0%–100%) and the distribution of oxide metals into the concentration (c) and the base (w). This study confirms that MGS is suitable for fine particles (+50 –100 µm), as demonstrated by [35] for Cu-Co oxides. Their recovery of ~85% for cobalt is comparable to the best tests in this study.

However, the observed variability (test 1 to test 7) suggests a strong dependence on operating parameters (rotation speed, tilt angle), which is consistent with the conclusions of [35] on the importance of hydrodynamic optimization [29]. The high Co_3O_4 content in (c), confirmed by high values, corroborates the work of [29], where MGS enabled efficient separation of Co from asbolane clays thanks to its adjustable centrifugal force.

In contrast, the residual Ni losses in (w) could be explained by a density similarity with gangues, a problem reported by [36] for nickel ores. The low MnO contents in (w) indicate good separation, consistent with the results of [37] on manganese ore separation with flotation of low-grade manganese ore using a novel linoleate hydroxamic acid. However, when Co_3O_4 or NiO persist in (w), additional steps (flotation, leaching) may be necessary, as proposed by [18,37–39].

3.7.2. Asbolane Mineral Concentrate Mass −50 µm

The asbolane mineral concentrate, ground to a particle size of 50 µm (finer than that shown in Figure 11), was subjected to seven metallurgical tests. The collected data include the metal recovery rates (%) as well as the chemical composition of the concentrate (c) and the tailings (w) in terms of MnO, Co_3O_4, and NiO.

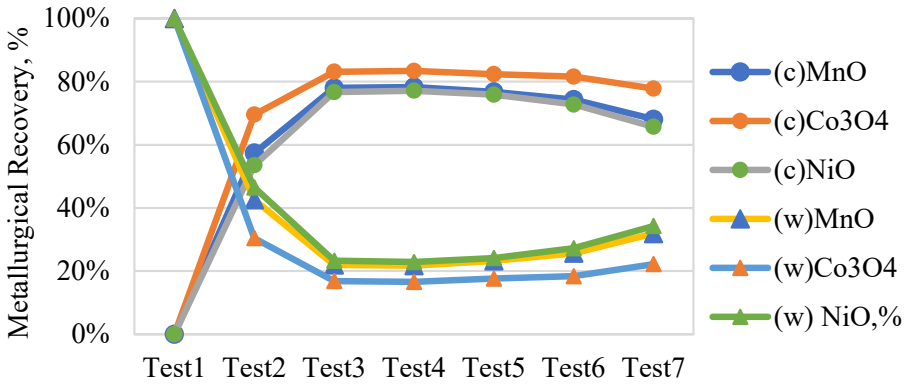

Figure 11. Metallurgical recovery: asbolane mineral concentrate mass—50 µm, where (c) is concentrate and (w) is residue (tailings).

Recovery ranges from 0% to 100%, with heterogeneous tests. The results suggest increased sensitivity to operating parameters for fine particles (50 µm) compared to 100 + 50 µm.

Ref. [40] demonstrated that the MGS is effective for particles smaller than 75 µm, but with decreased selectivity below 50 µm due to increased frictional forces. This explains the observed variability (test 1 to test 1 to 7).

The recovery of cobalt (Co_3O_4) and nickel (NiO) presents distinct challenges related to density differences and mineral associations.

Cobalt (Co_3O_4): The tests show high recoveries (>80%), which aligns with [37]'s work on asbolane, where MGS enabled effective separation due to the density difference between Co_3O_4 and the gangue. If losses persist in (w), this could be explained by Co-Mn micro-aggregates that are difficult to separate, as observed by [40].

Nickel (NiO): Low recoveries (Test 7 at 0%) could be due to the density similarity between NiO and residual silicates, a recurring issue reported by [41]. The analysis reveals that finer particles (50 µm) show greater results dispersion, highlighting the impact of particle size on the stability of MGS separation [39,40].

Finer particles (−50 µm) show a greater dispersion of results (82.4% Co_3O_4, 78.3% MnO, and 77.1% NiO), confirming that particle size influences the stability of MGS separation [37]. Optimizing hydrodynamic parameters (water flow, inclination angle) is crucial for fine particles, as recommended by [39].

The MGS remains suitable for fine ores rich in Co, with potential recoveries above 80% if the parameters are optimized. However, there are some challenges to overcome. The heterogeneity of the results highlights the need for strict control of the pulp, particularly its viscosity and solid content. Additionally, to address the loss of NiO, hybrid approaches, such as combining MGS with magnetic separation, could be tested, as suggested by [40].

This study on −50 µm asbolane reveals that MGS can achieve high cobalt recoveries, but with increased variability due to particle fineness. The challenges for nickel highlight the need for multifactorial approaches. These results line with recent work on the gravimetric separation of complex ores, while identifying key paths for optimizing processes at an industrial scale.

3.7.3. Asbolane Ore Recovery: Size Range −100 +50 µm

The distribution results of the percentage obtained in each of the seven asbolane tests are plotted in Figure 12. These values are compared with the value of ~1.3% of asbolane present in the overall mass of each bench-scale test in MGS, aiming for recovery in the −100 +50 µm fraction.

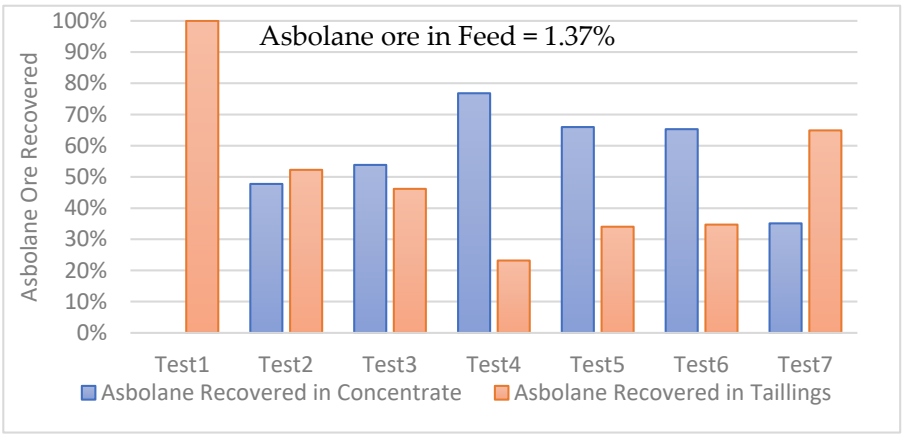

Figure 12. Asbolane recovery from Agios Ioannis laterites (asbolane content 1.37% and size range −100 +50 µm).

The data available seems to indicate the following conclusion:

Test 1: a 100% recovery of asbolane in the reject. This suggests a major significant problem in the separation process, where all of the target minerals were directed to the tailings instead of the concentrate. Several factors could explain this result, such as improper equipment settings, operational constraints (drum inclination × wash and water flow rate).

The tests 2 to 6 show variable recovery of asbolane in the concentrate, ranging from approximately 48% to 77%. This fluctuation indicates that operational parameters have a significant influence on separation efficiency. Furthermore, asbolane in the rejects throughout these tests highlights the difficulty in achieving complete separation.

Test 7 shows the lowest recovery in the concentrate, at only approximately 35%, and the highest recovery in the rejects, at approximately 65%. This result suggests that the conditions of this test were particularly unfavorable for the recovery of asbolane.

The consistent presence of asbolane in the rejects across all tests highlights the challenges associated with effectively separating this complex mineral. The feed particle size (−100 +50 μm) may have contributed to these difficulties, as coarser particles can retain locked asbolane grains.

The significant variation in recovery rates between tests highlights the importance of optimizing operational parameters. Centrifugal force, agitation frequency, tilt angle, and feed rate were controlled to maximize asbolane recovery.

3.7.4. Asbolane Ore Recovery: Size Range −50 μm

Figure 13 presents the results of the multi-stage concentration (MSG) tests for of asbolane (a cobalt–manganese mineral) in the −50 μm fraction. Asbolane ore in feed = 1.37%: the asbolane content in the feed ore was 1.37%. This relatively low content highlights the importance of efficient separation to recover asbolane.

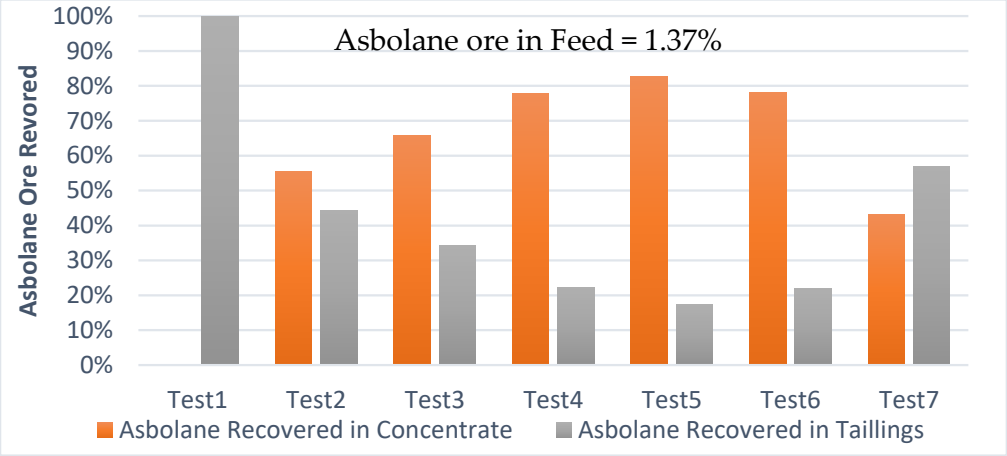

Figure 13. Asbolane recovery from Agios Ioannis laterites (asbolane content 1.37% and size range −50 μm).

The figure illustrates the results of seven tests (Tests 1 to 7) comparing asbolane recovery in two products: concentrate and tailings.

Test 1 shows a striking result with 100% recovery of asbolane in the rejects. As mentioned, this indicates a major problem in the separation process.

Tests 2 to 6 show variable recovery of asbolane in the concentrate, ranging from approximately 48% to 77% with more than 81% recovery in test 5. However, asbolane is also lost in the rejects, suggesting that the operational parameters were not optimal.

Test 7 shows the lowest recovery in the concentrate (~35%) and the highest recovery in the rejects (~65%), indicating ineffective separation.

The results in Figure 13 confirm the challenges associated with asbolane recovery from a sample with a particle size of −50 μm. As previously noted, feed particle size can on separation efficiency.

The variation in recovery rates between tests underscores the importance of optimizing operational parameters, such as centrifugal force, drum tilt angle, drum speed, and wash water, contributing to the overall performance.

The consistent loss of asbolane in the rejects across all tests indicates the need to explore other separation methods, such as flotation, to improve recovery.

The results confirm MSG's potential to recover substantial asbolane from low-grade feed, though further improvements are achievable through operational optimization, additional testing, and possibly integrating other separation methods. These results, with their significant proportions, have not been previously studied sufficiently and represent key paths for optimizing the process at an industrial scale, with consideration of the scale-up potential and cost-effectiveness of MGS implementation.

3.8. Particle Size Distribution

3.8.1. Size Range −100 +50 µm

Figure 14 illustrates the particle size distribution (PSD) results from seven separation tests on material within the −100 + 50 µm size range. Each subplot (a–g) represents a different test, reflecting how changes in process conditions affect separation outcomes.

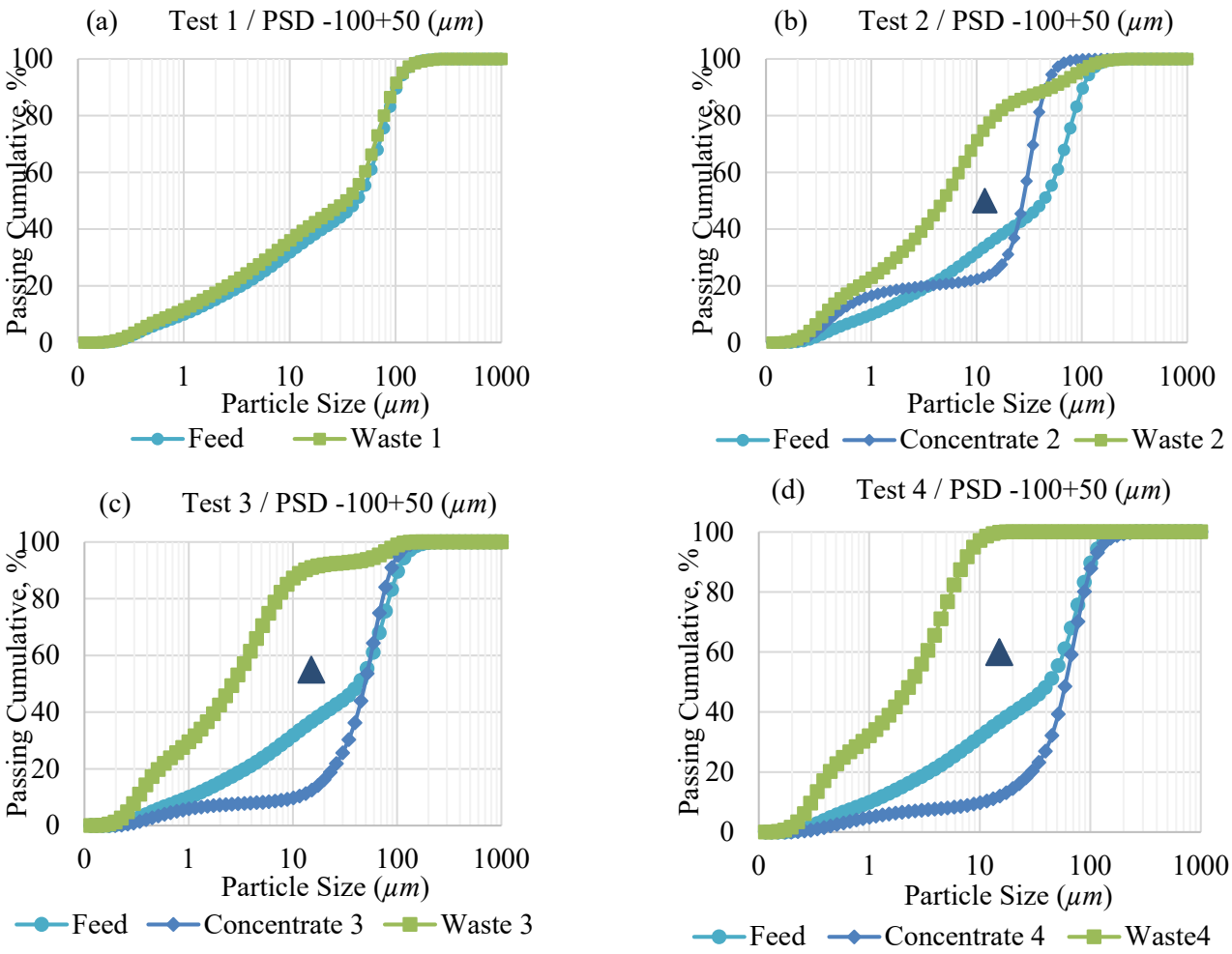

Figure 14. *Cont.*

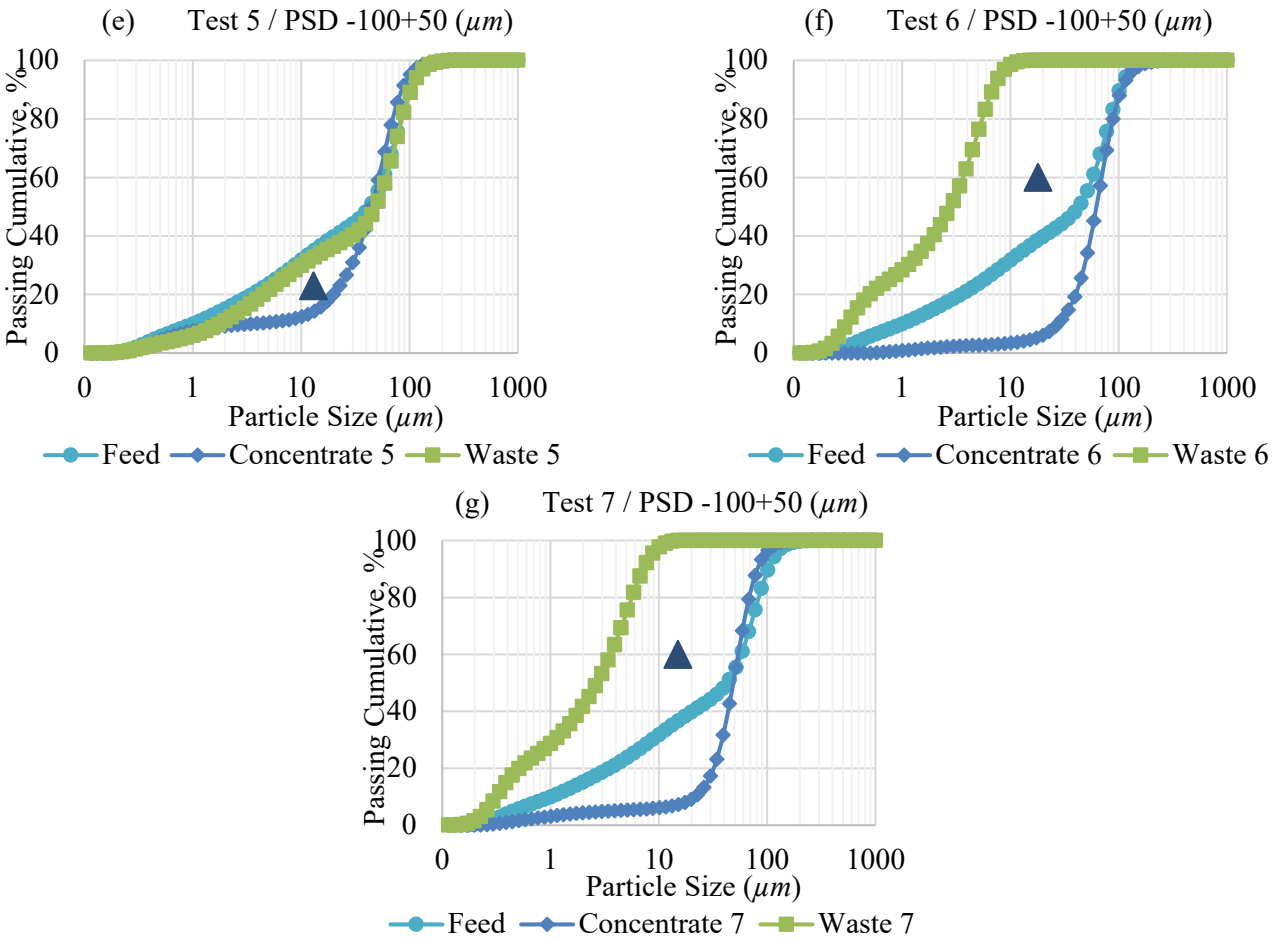

Figure 14. Particle size distribution (PSD) from laterites, Agios Ioannis. Size range −100 +50 μm, where (**a**) is test 1; (**b**) is test 2; (**c**) is test 3; (**d**) is test 4; (**e**) is test 5; (**f**) is test 6; and (**g**) is test 7.

The graphs display the cumulative percentage of particles passing for the feed, concentrate, and waste streams. The black triangles in each graph indicate the size range where separation was most effective, as the "separation zone". In this zone, the Multi-Gravity Separator (MGS) differentiates particles based on size and density.

This effective separation range arises from the interaction of various forces acting on particles inside the MGS, including gravity, centrifugal force, and fluid flow. These forces influence how particles with different densities and sizes are sorted.

The differences in the curves across the tests demonstrate how operating parameters, such as wash water rate and drum speed, can impact the efficiency of the process. For instance, a larger gap between the feed and concentrate curves typically indicates better separation performance and higher concentrate purity.

The cumulative particle size distribution (PSD) curves presented in Figure 14 offer a comparison of the particles passing through specific sieve sizes for the feed, concentrate, and tailings streams. The shape and displacement of each curve provide insight into the effectiveness of separation under varying operational conditions. Sharp inflection points, particularly those observed in test 4(d) marked by black triangles, highlight critical particle sizes where separation efficiency is maximized, especially for finer fractions in the −100 +50 μm range. In contrast, flatter and overlapping curves, such as those seen in test1(a), indicate poor selectivity and minimal differentiation between feed and concentrate distributions.

The displacement of the concentrate curve above the feed curve in specific tests, such as test 4(d), signifies the successful enrichment of finer particles within the product stream, demonstrating effective separation dynamics. Conversely, overlapping or minimally displaced curves suggest inadequate process conditions, where similar particle populations are retained in both streams. Tests 1 and 2 (a, b) further illustrate the favorable recovery of ultrafine particles (<50 μm), evidenced by the steep incline of concentrate curves in this region. However, recovery efficiency decreases for coarser fractions (>100 μm), reinforcing the particle size sensitivity of the separation process.

Variations in the morphology of the PSD curves are also linked to operational settings. Tests exhibiting enhanced separation performance, such as test 4(d), likely benefited from optimized parameters, such as higher wash water flow, increased drum rotation speed, or improved fluidization, all of which promote the preferential concentration of fine particles. In contrast, flatter profiles may be attributed to suboptimal hydraulic or mechanical conditions. These findings have important implications for process optimization: steeply rising concentrate curves suggest effective operational configurations (tilt angle, water flow rate, drum speed), while flatter or overlapping trends indicate opportunities to refine operational thresholds.

The results highlight the critical role of particle size in separation efficiency. In tests 1 and 2 (a and b), the recovery of fine particles is favorable. In contrast, other tests exhibit varying separation profiles, suggesting that further adjustments to process parameters may be necessary to optimize the recovery of desired particle sizes. The cumulative PSD curves reveal specific particle sizes more than others, reflecting the separation dynamics of the process. Better separation performance is observed in tests where the concentrate curve is higher than the feed (test 4(d)). In contrast, curves closer to the feed suggest less efficient recovery (e.g., Tests 1 and 2).

3.8.2. Range Particle −50 μm

Figure 15 shows the results of separation tests for particles down to −50 μm, with positive cumulative curves for feed, concentrate, and tailings. Each sub-figure (Figure 15a–g) represents a separate test, highlighting separation performance under different conditions. The black triangles explain the phenomenon described in the previous section, investigated in the size range of −100 to +50 microns.

The results indicate that the curves for tests 1 to 4 (a to d) show varied particle distributions, illustrating how size influences recovery in concentrates. Tests 5 and 6 (e and f) add dimension by presenting different processing configurations, while test 7 (g) explores an alternative method.

The results reveal that the separation of −50 μm particles is sensitive to processing conditions. In tests 1 and 2, the recovery of fine particles is satisfactory, indicating effective separation. However, tests 3 and 4 show variations in the shape of the curves, suggesting that adjustments to parameters, such as processing speed or water content, could improve performance.

The black triangles on the curves represent points of optimal separation, indicating specific particle sizes that can be better recovered. The tailings curves also show significant trends, illustrating how unwanted particles are removed from the concentrate.

When comparing these results with those from tests on −100 +50 μm particles, it is clear that particle size has a significant impact on separation dynamics. Tests on −50 μm particles generally show higher recovery in the concentrates, which can be attributed to the reduced particle size, thereby facilitating separation. However, this increased efficiency is accompanied by potential complexity in tailings management, as finer size can lead to greater concentrate contamination.

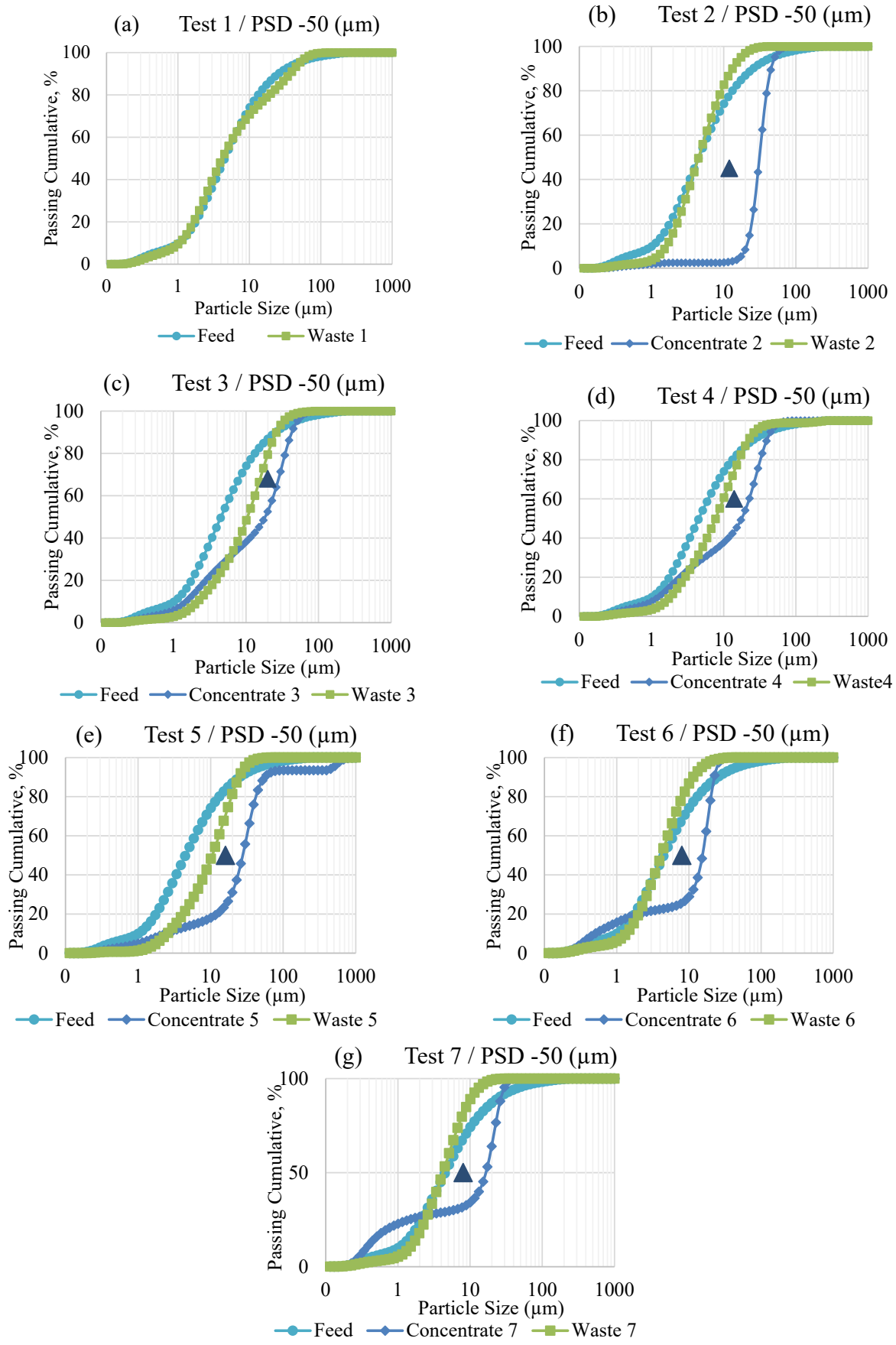

Figure 15. Particle size distribution (PSD) from laterites with a particle range −50 µm in (**a**) test 1; (**b**) test 2; (**c**) test 3; (**d**): test 4; (**e**) test 5; (**f**) test 6; and (**g**) test 7.

Although −50 μm particles offer advantages in terms of recovery, they require greater attention to operational parameters to avoid losses in the final concentrate. Strategic adjustments based on these results could enable the significant optimization of separation processes, both for fine and coarser particle sizes.

4. Conclusions

This study demonstrates that the Multi-Gravity Separator is highly effective for fine particles, producing wonderful asbolane particles. The following key conclusions can be drawn from the research:

- Operational parameters strongly influence asbolane recovery by the MGS.
- The feed pulp solids ratio (x_1), drum speed (x_2), drum tilt angle (x_3), and wash water flow rate (x_4) significantly affect both the recovery and grade of the asbolane concentrate.
- Although optimization was not conducted, results suggest that refining operational parameters may improve separation efficiency and asbolane recovery in future continuous tests.
- Proper optimization of these factors helps reduce the loss of valuable minerals such as cobalt (Co), manganese (Mn), and nickel (Ni).
- In the Agios Ioannis laterite, the recovery of asbolane from the −50 μm fraction reached 81.2%, while the −100 +50 μm fraction achieved approximately 76% recovery.
- The particle size data shown that MGS provides a cut in particle with −10 μm diameter to indicate that MGS achieves a reduction in particle size with a −10 μm diameter in the tailings, respectively.

These results highlight the significance of fine-tuning the operational parameters of the MGS process to improve recovery and minimize mineral loss, ultimately enhancing the overall efficiency of asbolane concentration. While this study presents essential and novel results, additional research is needed to explore alternative separation methods, such as flotation, to optimize asbolane recovery further.

Author Contributions: Conceptualization, A.E. and J.O.M.; Methodology, C.H.S.; Software, M.M.V.; Validation, A.E., M.M.V., C.H.S., J.O.M. and S.T.; Formal analysis, M.M.V. and C.H.S.; Investigation, A.E.; Resources, S.T. and J.L.C.P.; Data curation, M.M.V. and J.L.C.P.; Writing—original draft, A.E.; Writing—review & editing, C.H.S.; Visualization, M.M.V.; Supervision, A.E., C.H.S. and J.O.M.; Project administration, S.T. and J.L.C.P.; Funding acquisition, J.O.M., S.T. and J.L.C.P. All authors have read and agreed to the published version of the manuscript.

Funding: This research was funded by the following project: 101091682-Metallico-HORIZON-CL4-2022-RESILIENCE-01.

Data Availability Statement: Data are contained within the article.

Acknowledgments: The authors thank the company GMMSA Larco for the samples provided. This work was supported by the METALLICO project and by the development of upcycling approaches in the agri-food and process industries to promote on-site and sustainable chemicals production (Upcycling) project (PID2023-147160OB-C21), financed by the Spanish Research Agency (Agencia Estatal de Investigación, AEI).

Conflicts of Interest: The authors declare no conflicts of interest.

References

1. Mudd, G.M. Global trends and environmental issues in nickel mining: Sulfides versus laterites. *Ore Geol. Rev.* **2010**, *38*, 9–26. [CrossRef]
2. Dalvi MKlauber, C.; Robinson, T. A study into the behaviour of nickel, cobalt and metal impurities during the atmospheric pressure leaching of a limonitic laterite ore. *Hydrometallurgy* **2004**, *74*, 241–257.
3. Kanungo, M.; Mishra, K.G.; Das, S.C. Study on morphology of copper deposited onto aluminium by immersion plating from an oxalate bath containing perchloric acid. *Miner. Eng.* **2003**, *16*, 1383–1386. [CrossRef]
4. Farrokhpay, S.; Fornasiero, D. Flotation of coarse composite particles: Effect of mineral liberation and phase distribution. *Adv. Powder Technol.* **2017**, *28*, 1849–1854. [CrossRef]
5. Mäkinen, J.; Bachér, J.; Kaartinen, T.; Wahlström, M.; Salminen, J. The effect of flotation and parameters for bioleaching of printed circuit boards. *Miner. Eng.* **2015**, *75*, 26–31. [CrossRef]
6. Eljoudiani, A.; Sampaio, C.H.; Oliva, J.; Veras, M.M.; Alfonso, P.; Anticoi, H.; Tampouris, S.; Cortina, J.L.; Escalante, P.R. Technological Characterization of Cobalt and Nickel Ores from Greece for Metal Recovery. *Separations* **2024**, *11*, 345. [CrossRef]
7. Petruk, W. *Applied Mineralogy in the Mining Industry*; Elsevier BV: Amsterdam, The Netherlands, 2000; p. 288.
8. AI-Khirbash, S.A. Mineralogical characterization of low-grade nickel laterites from the North Oman Mountains: Using mineral liberation analyses—Scanning electron microscopy-based automated quantitative mineralogy. *Ore Geol. Rev.* **2020**, *122*, 1–10. [CrossRef]
9. Quast, K.; Otsuki, A.; Fornasiero, D.; Robinson, D.J.; Addai-Mensah, J. Preconcentration Strategies in the Processing of Nickel Laterite Ores Part 3: Flotation Testing. *Miner. Eng.* **2015**, *79*, 279–286. [CrossRef]
10. Program (Co-ISRTP). Cobalt Institute. Available online: https://www.cobaltinstitute.org/ (accessed on 28 May 2025).
11. Al-Khirbash, S. Genesis and Mineralogical Classification of Ni-Laterites, Oman Mountains. *Ore Geol. Rev.* **2015**, *65*, 199–212. [CrossRef]
12. Dutrizac, J.E.; MacDonald, R. Processing of Nickel Laterite Ores on the Rise. *Min. Eng.* **2019**, *71*, 45–51.
13. Santos, A.L.; Dybowska, A.; Schofield, P.F.; Herrington, R.J.; Cibin, G.; Johnson, D.B. Chromium (VI) Inhibition of Low pH Bioleaching of Limonitic Nickel-Cobalt Ore. *Front. Microbiol.* **2022**, *12*, 802991. [CrossRef]
14. Honaker, R.Q.; Patil, D.P. Application of Multi-Gravity Separator for Beneficiation of Nickel and Cobalt Ores. *Miner. Eng.* **2002**, *15*, 523–528. [CrossRef]
15. Bulatovic, S.M. Flotation of Rare Earth Minerals from Silicate–Hematite Ore Using Tall Oil Fatty Acid. *Miner. Eng.* **2010**, *23*, 1231–1238. [CrossRef]
16. Das, S.; Sarkar, S. Advanced Gravity Separators-A Review of State of the Art Technology. *Miner. Process. Extr. Metall. Rev.* **2016**, *37*, 85–105.
17. Zhang, L.; Khoso, S.; Tian, M.; Sun, W. Cassiterite Recovery from a Sulfide Ore Flotation Tailing by Combined Gravity and Flotation Separations. *Physicochem. Probl. Miner. Process.* **2020**, *57*, 206–215. [CrossRef]
18. Wills, B.A.; Finch, J.A. *Wills' Mineral Processing Technology: An Introduction to the Practical Aspects of Ore Treatment and Mineral Recovery*, 8th ed.; Butterworth-Heinemann: Oxford, UK, 2016.
19. Emmanuel, A.; Zisis, D.; Adam, K. Magnetic Gravity Separation for the Recovery of Cobalt and Nickel from Lateritic Ores. *Minerals* **2021**, *11*, 1279. [CrossRef]
20. Nzeh, N.S.; Popoola, P.; Adeleke, A. Physicochemical concentration of heavy minerals-a treatise on wet process media: Gravity, centrifugal, and flotation techniques. *Int. J. Min. Miner. Eng.* **2024**, *15*, 161–236. [CrossRef]
21. Falconer, S.T. The multi-gravity separator: A review of recent applications. *Miner. Eng.* **2003**, *16*, 1083–1091. [CrossRef]
22. Goktepe, F. Multi-gravity separator applications and operational parameters. *Miner. Eng.* **2005**, *18*, 1195–1203.
23. Gravity Mining Ltd. How the Gravity Mining-Multi Gravity Separator Works. Available online: https://www.gravitymining.com (accessed on 28 May 2025).
24. Montgomery, D.C. Applications of design of experiments in engineering. *Qual. Reliab. Eng. Int.* **2008**, *24*, 501–502. [CrossRef]
25. Box, G.E.P.; Draper, N.R. *Response Surfaces, Mixtures, and Ridge Analyses*, 2nd ed.; Wiley-Interscience: Hoboken, NJ, USA, 2007. [CrossRef]
26. Burt, R.O. *Gravity Concentration*; Springer: Dordrecht, The Netherlands, 2001. [CrossRef]
27. Kursun ODeveci, H.; Goktepe, F. Gravity separation of cobalt from asbolane clay using a multi-gravity separator. *Sep. Sci. Technol.* **2019**, *54*, 1845–1855.
28. Falconer, A. Gravity Separation: Old Technique/New Methods. *Phys. Sep. Sci. Eng.* **2003**, *12*, 31–48. [CrossRef]
29. Han, Y.; Fan, M.; Yu, J.; Wang, C.; Cao, Y. The flotation of low-grade manganese ore using a novel linoleate hydroxamic acid. *Colloids Surf. A: Physicochem. Eng. Aspects.* **2015**, *466*, 1–9. [CrossRef]
30. Zappala, L.; McDonald, R.; Powncebyc, M.I. Nickel Laterite Beneficiation and Potential for Upgrading Using High Temperature Methods: A Review. *Miner. Process. Extr. Metall. Review.* **2023**, *45*, 767–789. [CrossRef]

31. Xu, P.; Wang, Q.; Li, C.; Yu, Q.; Fang, H.; Su, J.; Guo, X. Relationship between process mineralogical characterization and beneficiability of low-grade laterite nickel ore. *J. Cent. South Univ.* **2021**, *28*, 3061–3073. [CrossRef]
32. Chaurasia, R.C.; Panwar, D.S.; Ken, B.S.; Mehta, J.; Oza, A.D.; Kumar, S.; Panwar, D.S.; Ken, B.S.; Mehta, J.; Oza, A.D.; et al. Enhancing gravity separation for improved mineral processing. *Multidiscip. Sci. J.* **2024**, *7*, e2025190. [CrossRef]
33. Chan, W.T.; Evans, N.E.; Bradshaw, D.J. Multi-gravity separation of copper-cobalt oxides from a complex ore. *Miner. Eng.* **2020**, *150*, 106297.
34. Tripathy, S.K.; Murthy, Y.R.; Singh, V.; Farrokhpay, S.; Filippov, L.O. Improving the quality of ferruginous chromite concentrates via physical separation methods. *Minerals* **2019**, *9*, 667. [CrossRef]
35. Tripathy SKSKDas, B.; Kumar, V. Optimization of multi-gravity separator for the beneficiation of low-grade iron ore. *Trans. Indian Inst. Met.* **2018**, *71*, 3023–3032.
36. Alajoki, J.; Karppinen, A.; Rinne, T.; Serna-Guerrero, R.; Lundström, M. Leaching strategies for the recovery of Co, Ni, Cu, and Zn from historical flotation tailings. *Miner. Eng.* **2024**, *217*, 108967. [CrossRef]
37. Das, S.; Sarkar, S. Characterization and Feasible Physical Separation Methods for Processing of Yxsjöberg Tungsten Ore Tailings. *Miner. Process. Extr. Metall. Rev.* **2019**, *40*, 111–126.
38. Dutta, D.; Kumari, A.; Panda, R.; Jha, S.; Gupta, D.; Goel, S.; Jha, M.K. Closed-loop separation process for recovering Co, Cu, Mn, Fe, and Li from spent lithium-ion batteries. *Sep. Purif. Technol.* **2018**, *210*, 690–698. [CrossRef]
39. Das, S.; Sarkar, S. Advanced Gravity Concentration of Fine Particles: A Review. *Miner. Process. Extr. Metall. Rev.* **2018**, *39*, 225–246. [CrossRef]
40. Cheng, C.; Boddy, G.; Zhang, W.; Godfrey, W.; Barnard, M.; Robinson, K.; Pranolo, D.; Zhu, Y.; Zeng, Z.; Wang, L.; et al. Separating nickel and cobalt from manganese, magnesium, and calcium by synergistic solvent extraction—from batch tests to pilot plant operation. *Hydrometallurgy* **2015**, *156*, 1–10. [CrossRef]
41. Bruckard, W.J.; Muir, D. A New Process for Cobalt–Nickel Separation. In Proceedings of the International Symposium on Hydrometallurgy, Phoenix, AZ, USA, 27–30 August 2023; pp. 1–9.

Disclaimer/Publisher's Note: The statements, opinions and data contained in all publications are solely those of the individual author(s) and contributor(s) and not of MDPI and/or the editor(s). MDPI and/or the editor(s) disclaim responsibility for any injury to people or property resulting from any ideas, methods, instructions or products referred to in the content.